

# Modelling galaxy clustering at high redshift

Lauro Moscardini<sup>1</sup>, Peter Coles<sup>2</sup>, Francesco Lucchin<sup>1</sup> and Sabino Matarrese<sup>3</sup>

<sup>1</sup>*Dipartimento di Astronomia, Università di Padova, vicolo dell'Osservatorio 5, I-35122 Padova, Italy*

<sup>2</sup>*Astronomy Unit, School of Mathematical Sciences, Queen Mary & Westfield College, Mile End Road, London E1 4NS*

<sup>3</sup>*Dipartimento di Fisica G. Galilei, Università di Padova, via Marzolo 8, I-35131 Padova, Italy*

2 December 2024

## ABSTRACT

We discuss the theoretical interpretation of observational data concerning the clustering of galaxies at high redshifts. Building on the theoretical machinery developed by Matarrese et al. (1997), we make detailed quantitative predictions of galaxy clustering statistics for a variety of cosmological models, taking into account differences in spatial geometry and initial fluctuation spectra and exploring the role of bias as a complicating factor in these calculations. We compare these predictions with current observational data to constrain available models. Theories of structure formation that fit the present-day abundance of rich clusters are generally compatible with the observed redshift evolution of galaxy clustering if galaxies are no more than slightly biased at  $z \sim 1$ . We also discuss the interpretation of a concentration of Lyman-break galaxies found by Steidel et al. (1997), coming to the conclusion that such concentrations are not unexpected in ‘standard’ models of structure formation.

**Key words:** cosmology: theory – cosmology: observations – large-scale structure of Universe – galaxies: formation – galaxies: evolution – galaxies: haloes

## 1 INTRODUCTION

The direct observation of statistically complete samples of galaxies at high redshift has only recently become technologically feasible, but it promises to yield important information about the origin and evolution of cosmic structures. In particular, the possibility to observe “normal” galaxies (or their progenitors), rather than just quasars or other ultraluminous sources, may lead to an understanding of how these objects relate to the distribution of the dark matter which is assumed, in most theories, to dominate the density of the Universe. This, in turn, should allow observations of galaxy clustering to be used to gain insights about fundamental aspects of cosmological models, as well as learning about the way galaxies themselves evolve. But in this field, theory currently lags considerably behind observations, with the result that experimental data are sometimes placed in a naive, or perhaps simply incorrect, theoretical context.

In Matarrese et al. (1997; hereafter Paper I), we discussed high-redshift clustering phenomena from a theoretical perspective. In particular, we developed a general formalism which one can use to make detailed predictions of statistical measures of clustering and which also makes explicit the main sources of theoretical uncertainty in these predictions. This formalism allows one to make a realistic assessment of how models of structure formation fare in the face of results from particular observational programmes. This formalism is considerably more complicated than the usual simple scaling ansatz which forms the framework within which most observational results have previously been interpreted.

It is the main purpose of this paper to deploy the techniques of Paper I in a systematic comparison of currently popular structure formation models with the available observational data. The models are all based on the cold dark matter (CDM) model, but vary in the amount of dark matter, the initial perturbation spectrum, the background cosmology and in the presence or absence of a cosmological constant. These variations have been introduced in an attempt to reconcile the basic idea of CDM with cosmological observations which rule out the simplest version of the model; see, e.g. Coles (1996). This detailed comparison requires us to specify the assumptions entering our calculations very carefully, so we also take the opportunity to refine the general arguments we made in Paper I.

The layout of the paper is as follows. In Section 2, we briefly recap the main elements of the approach outlined in Paper I and explain the extension to, for example, the case of an open universe or models with cosmological constant. We also describe the six models of structure formation we use to compare with the data. We explore the issue of bias in Section 3, drawing on some themes that were introduced in Paper I, but focussing on the specific case of galaxy formation in hierarchical clustering models. Section 4 contains a critique of some simple theoretical arguments often presented in the literature. The detailed comparison of clustering observations with our theoretical predictions is made in Section 5, where the relevant data are also described. We also comment on the theoretical interpretation of a concentration of galaxies found at redshift  $\sim 3$  by Steidel et al. (1997). We present our main conclusions in Section 6.

## 2 MODELLING THE EVOLUTION OF CLUSTERING

### 2.1 Preliminaries

In order to model the clustering of high-redshift galaxies, and to compare observational data with the predictions of different cosmological models, one must confront a number of different issues. Firstly, there is the necessity to have a reliable way to follow the redshift evolution of matter correlations. Secondly, one has to model the relationship between fluctuations in the mass and fluctuations in observable galaxies, and to consider the possible time evolution of this relationship. In the usual language, this means devising a model for the *bias*. Another ingredient is the calculation of effects introduced by the observing process, such as the role of the selection function, and the possible effect of redshift-space distortions on measures of clustering. Finally, because of the limited number of galaxies in available samples and the need to obtain a reasonable statistical signal-to-noise ratio, observational results are usually presented for galaxies spanning a range of redshifts. This last effect means, for example, that the observed correlation function of the sample involves a convolution of the real correlation function with the redshift distribution of the objects contained in the sample.

We should also point out that gravitational lensing effects along the observer's past light cone also introduce a bias into the observed statistics (e.g. Villumsen 1996; Moessner, Jain & Villumsen 1997). The presence of a correlated shear results in increased apparent clustering over and above that produced by the intrinsic galaxy correlations. Likewise the distortion introduced by inferring galaxy positions from redshifts also acts to increase clustering statistics with respect to the real-space versions, except for projected correlations which do not suffer from this effect. Since these effects both act in the same direction, calculations made without taking them into account are not exactly comparable with observations: more realistic predictions, however, would always be higher than those we present here.

In Paper I we developed a formalism that takes into account all these requirements, and most of this section is devoted to a brief summary of the machinery that was constructed there. Essentially, Paper I showed that the observed correlation function  $\xi_{\text{obs}}$  in a given redshift interval  $\mathcal{Z}$  is an appropriate weighted average of the mass autocorrelation function  $\xi$  with the mean number of objects  $N$  and effective bias factor  $b_{\text{eff}}$ , defined below in equation (3), in that range:

$$\xi_{\text{obs}}(r) = N^{-2} \int_{\mathcal{Z}} dz_1 dz_2 \mathcal{N}(z_1) \mathcal{N}(z_2) b_{\text{eff}}(z_1) b_{\text{eff}}(z_2) \xi(r, \bar{z}), \quad (1)$$

where  $N \equiv \int_{\mathcal{Z}} dz' \mathcal{N}(z')$  and  $\bar{z}$  is an intermediate redshift between  $z_1$  and  $z_2$ . Porciani (1997), by computing the evolution of the two-point correlation function in the Zel'dovich (1970) approximation, showed that adopting the relation  $D_+(\bar{z}) = \sqrt{D_+(z_1)D_+(z_2)}$ , where  $D_+$  is the growth law for linear density fluctuations (see below, Section 2.4), ensures that predictions will be accurate to an error smaller than 1 per cent. In the following we will assume this expression to define  $\bar{z}$ .

### 2.2 Bias and all that

The factor of  $b_{\text{eff}}$  which appears in equation (1) is a consequence of our lack of understanding of the details of the galaxy formation process and the consequently uncertain relationship between fluctuations in matter density  $\delta_m$  and galaxy number-density  $\delta_n$ . It is conventional to parametrise one's ignorance in this arena by introducing a single linear *bias parameter* such that a relationship of the form  $\delta_n = b \delta_m$  is assumed. In this work we shall generalise this idea so that we assume that objects with given intrinsic properties (such as mass  $M$ ) and at different redshifts  $z$  can have different bias parameters, which we call  $b(M, z)$ . For each set of objects, however, the bias is assumed still to be linear; it is also *local*, in the sense that the propensity of galaxies to form at a given spatial location  $\mathbf{x}$  depends only on the matter density at that point:

$$\delta_n(\mathbf{x}; M, z) \simeq b(M, z) \delta_m(\mathbf{x}, z); \quad (2)$$

so that no environmental or co-operative effects in galaxy formation are permitted. If we assume such a bias between the galaxy and mass fluctuations, the *effective* bias factor  $b_{\text{eff}}(z)$  which appears in equation (1) can be expressed as a suitable average of the “monochromatic” bias  $b(M, z)$  (i.e. the bias factor of each single object):

$$b_{\text{eff}}(z) \equiv \mathcal{N}(z)^{-1} \int_{\mathcal{M}} d \ln M' b(M', z) \mathcal{N}(z, M'). \quad (3)$$

Here the variable  $M$  (and its range  $\mathcal{M}$ ) does not necessarily simply represent the object’s mass but rather it stands for any generic intrinsic properties of the object (mass, luminosity, etc.) on which the selection of the object into an observational sample might depend.

Because it plays such an important role in this formalism, we have devoted the whole of Section 3 to a more detailed discussion of the possible form of a bias and its redshift evolution.

### 2.3 Clustering Statistics

Owing to the relatively small size of the datasets available at the present time, clustering properties of high-redshift galaxies are generally studied in terms of the angular  $[\omega_{\text{obs}}(\vartheta)]$  or of the projected real-space  $[w_{\text{obs}}(r_p)]$  correlation functions. Adopting the *small-angle* approximation, in Paper I we obtained for  $\omega_{\text{obs}}$ :

$$\omega_{\text{obs}}(\vartheta) = N^{-2} \int_{\mathcal{Z}} dz G(z) \mathcal{N}^2(z) b_{\text{eff}}^2(z) \int_{-\infty}^{\infty} du \xi[r(u, \vartheta, z), z], \quad (4)$$

where  $r(u, \vartheta, z) \equiv a_0 \sqrt{u^2 + x^2(z) \vartheta^2}$ , with  $x(z)$  given by

$$x(z) = \frac{c}{H_0 a_0 \sqrt{|\kappa|}} \mathcal{S} \left( \sqrt{|\kappa|} \int_0^z \left[ (1+z')^2 (1 + \Omega_{0m} z') - z' (2 + z') \Omega_{0\Lambda} \right]^{-1/2} dz' \right) \quad (5)$$

and

$$G(z) \equiv \left( \frac{dx}{dz} \right)^{-1}. \quad (6)$$

In equation (5) and hereafter, we use  $\Omega_{0m}$  and  $\Omega_{0\Lambda}$  to represent the contribution at the present time to a critical energy density from matter and vacuum energy respectively. When we require these quantities at an arbitrary time we use  $\Omega_m$  and  $\Omega_\Lambda$ ; since they evolve with epoch,  $\Omega_m$  and  $\Omega_\Lambda$  are implicit functions of  $z$ ; although the cosmological constant  $\Lambda$  is constant in redshift,  $\Omega_\Lambda = \Lambda/3H^2$ , which varies through the Hubble constant  $H(z)$ . We write the total density parameter  $\Omega_m + \Omega_\Lambda \equiv \Omega_t$ ; consequently  $\Omega_{0m} + \Omega_{0\Lambda} = \Omega_{0t}$ .

Note also that, while in the Einstein–de Sitter case  $a_0$  is an arbitrary length–scale which can be set to unity, in the non–flat case it is given by

$$a_0 = \frac{c}{H_0} |1 - \Omega_{0t}|^{-1/2}. \quad (7)$$

In equation (5), if  $\Omega_{0t} < 1$ ,  $\mathcal{S}(x) \equiv \sinh(x)$  and  $\kappa = 1 - \Omega_{0t}$ ; if  $\Omega_{0t} > 1$ ,  $\mathcal{S}(x) \equiv \sin(x)$  and  $\kappa = 1 - \Omega_{0t}$ ; if  $\Omega_{0t} = 1$ ,  $\mathcal{S}(x) \equiv x$  and  $\kappa = 1$ . In the case of a vanishing cosmological constant, the previous expression can be solved analytically and can be written as

$$x(z) = \frac{2c}{a_0 H_0} \frac{\Omega_{0m} z + (\Omega_{0m} - 2)[-1 + (\Omega_{0m} z + 1)^{1/2}]}{\Omega_{0m}^2 (1 + z)}. \quad (8)$$

The *projected* real–space correlation function  $w_{\text{obs}}$  can be directly obtained by  $\xi_{\text{obs}}(r)$  as

$$w_{\text{obs}}(r_p) = 2 \int_0^\infty dy \xi_{\text{obs}}(\sqrt{r_p^2 + y^2}) = 2 \int_{r_p}^\infty dr r (r^2 - r_p^2)^{-1/2} \xi_{\text{obs}}(r), \quad (9)$$

where  $r_p$  is the component of the pair separation perpendicular to the line of sight.

### 2.4 Evolution of the mass autocorrelation function

The non-linear growth of the density fluctuations modifies the shape of the power spectrum  $P(k)$  as well as its amplitude. In the linear regime, which holds at large scales and/or early times, the solution is given by the relation

$$P(k, z) = D_+^2(z) P(k, z = 0), \quad (10)$$

where  $D_+(z)$  is the growing mode of linear perturbations normalised to unity at  $z = 0$ , so that the spectrum grows with time without any change in shape. By contrast, in the strongly non-linear regime, some theoretical arguments and numerical simulation results suggest the existence of the so-called stable clustering regime wherein the matter correlations exhibit a particular form of self-similar behaviour (Peebles 1980; Jain, Mo & White 1995; Jain 1997), although whether the stable clustering description holds in detail is still open to some doubt (e.g. Padmanabhan et al. 1996; Munshi et al. 1997). We shall return to this issue later, in Section 4 of this paper. In any case, the non-linear behaviour of matter correlations on small scales results in a distortion of the shape of the matter power spectrum from its initial form.

The clustering behaviour which is most relevant to the study of objects at high redshift is actually in between these two extremes. This intermediate regime is generally studied by fitting results from numerical simulations with a semi-empirical universal function, obtained by following the simple *ansatz* originally introduced by Hamilton et al. (1991). Recognising that gravitational collapse changes the effective length scale of a density perturbation, Hamilton et al. (1991) suggested that the initial (linear) scale  $r_0$  of a density perturbation should be related to the final (non-linear) scale  $r$  of the same perturbation after collapse by:

$$r_0 = [1 + \bar{\xi}(r, z)]^{1/3} r, \quad (11)$$

where

$$\bar{\xi}(r, z) \equiv \frac{3}{r^3} \int_0^r y^2 \xi(y, z) dy \quad (12)$$

is the integrated correlation function. The Hamilton et al. idea is that there is a universal function  $F$  acting on  $\bar{\xi}$ , once the change in appropriate length scale is taken into account:

$$\bar{\xi}(r, z) = F[\bar{\xi}_{\text{lin}}(r_0, z)]. \quad (13)$$

Recently this formalism has been significantly refined and generalised. Peacock & Dodds (1994) considered the application of this method to the power spectra rather than the correlation function, and also to models with arbitrary background density (i.e. with  $\Omega_{0t} \neq 1$  or  $\Omega_{0\Lambda} \neq 0$ ). Jain, Mo & White (1995) introduced the dependence of the universal function  $F$  of the primordial spectral index  $n$ . Finally Peacock & Dodds (1996, hereafter PD96), by using N-body simulations with high spatial resolution, obtained accurate fits for  $F$  both in low-density universes and universes with non-vanishing cosmological constant. The accuracy of this form of the fitting function has been recently confirmed using numerical experiments by Jenkins et al. (1997).

In Paper I we followed the clustering evolution by using the fitting function obtained by Jain, Mo & White (1995). Here, because it is our intention to consider models with  $\Omega_{0t} \neq 1$  or  $\Omega_{0\Lambda} \neq 0$ , we have decided instead to use the form of the method presented by PD96 which deals with the (dimensionless) power spectrum  $\Delta^2$ :

$$\Delta^2(k) \equiv \frac{d\sigma^2}{d \ln k} = \frac{1}{2\pi^2} k^3 P(k), \quad (14)$$

which is related to the two-point correlation function by

$$\xi(r) = \int \Delta^2(k) \frac{\sin kr}{kr} \frac{dk}{k}; \quad (15)$$

$\sigma^2$  is the variance of the density fluctuation field. In this case, the corresponding expressions for equations (13) and (11) are:

$$\Delta^2(k, z) = \mathcal{F}[\Delta_{\text{lin}}^2(k_0, z)], \quad k_0 = [1 + \Delta^2(k, z)]^{-1/3} k, \quad (16)$$

where  $k_0$  and  $k$  are the linear and non-linear wavenumbers, respectively. The universal fitting function adopted by PD96 is

$$\mathcal{F}(x) = x \left[ \frac{1 + B\beta x + [Ax]^{\alpha\beta}}{1 + ([Ax]^{\alpha} g^3 / [Vx^{1/2}])^{\beta}} \right]^{1/\beta}, \quad (17)$$

where  $g$  is a suppression factor that measures the rate of clustering growth in a particular cosmology relative to that which pertains in a flat matter-dominated Universe. The quantity  $g$  therefore contains a dependence on the background cosmology. Carroll, Press & Turner (1992) found an approximate (but almost exact) expression for  $g$ :

$$g(\Omega_m, \Omega_{\Lambda}) = \frac{5}{2} \Omega_m [\Omega_m^{4/7} - \Omega_{\Lambda} + (1 + \Omega_m/2)(1 + \Omega_{\Lambda}/70)]^{-1}. \quad (18)$$

Since  $\Omega_m$  and  $\Omega_{\Lambda}$  both depend upon redshift  $z$  (e.g. Section 2.3), and it is the dependence of  $g$  on  $z$  in which we are interested, we can use  $g(z)$  to encode this behaviour for any particular cosmological model. The formula given for

$\mathcal{F}$  above was given originally for  $z = 0$  by PD96, but it applies at any cosmic epoch  $z$  by replacing  $g$  by  $g(z)$ . The quantity  $x$  must also be interpreted as the linear power spectrum at the epoch  $z$ , i.e.

$$x = \Delta_{\text{lin}}^2(k_0, z) = \Delta_{\text{lin}}^2(k_0, z = 0)(1 + z)^{-2}[g(z)/g(0)]^2, \quad (19)$$

rather than at  $z = 0$  which is assumed in the original PD96 application. The parameters of the function  $\mathcal{F}(x)$  and their dependence on the spectral index  $n$  were obtained by fitting the results of N-body simulations. PD96 obtained:

$$A = 0.482(1 + n/3)^{-0.947}, \quad (20)$$

$$B = 0.226(1 + n/3)^{-1.778}, \quad (21)$$

$$\alpha = 3.310(1 + n/3)^{-0.244}, \quad (22)$$

$$\beta = 0.862(1 + n/3)^{-0.287} \quad (23)$$

and

$$V = 11.55(1 + n/3)^{-0.423}. \quad (24)$$

The previous expressions hold for power-law spectra. For models which are not described by pure power-law spectra, such as the variations on the cold dark matter model that we shall discuss in this paper, one can use the same formulae, but replacing  $n$  by an effective index  $n_{\text{eff}}$ , defined by

$$n_{\text{eff}}(k_0, z) = \left. \frac{d \ln P_{\text{lin}}(k, z)}{d \ln k} \right|_{k=k_0(z)/2}. \quad (25)$$

PD96 claim that this prescription is able to reproduce the non-linear evolution with a precision of about 7 per cent, which is perfectly adequate for the application we have in mind for this paper.

Some care has to be taken if one seeks to apply the PD96 method to cosmological models where  $\Delta^2$  displays a significant peak at some particular wavenumber. Such models are not really consistent with the assumption of hierarchical clustering in the first place. For example, tilted cold dark matter models have  $n_{\text{eff}} < -3$  for large  $k$ , which means that they have a very sharp spectral feature and are susceptible to this difficulty (see e.g. Vittorio, Matarrese & Lucchin 1988). Of course, the method can still be used to construct the power spectra on large scales and it is possible to use safely its predictions down to the linear wavenumber where the spectrum peaks. For many variants of tilted cold dark matter models (as those described in the following subsection),  $\Delta^2$  is sufficiently large there that the non-linear power will be very large. One would not want to make predictions based solely on dark matter clustering to any smaller scales, so the fact that  $n_{\text{eff}} < -3$  on the smallest linear scales is not a problem in the context of this work.

## 2.5 The cosmological models

One of the limitations of Paper I was that it restricted attention to a simple phenomenological model of the initial power spectrum and to a flat spatial geometry. It is one of the aims of this paper to extend the treatment to study a wider range of initial conditions and relevant changes in the global cosmological parameters (including spatial curvature). This is a particularly interesting task at the present time because it is well known that the so-called standard cold dark matter (SCDM) model — which assumes a flat universe with  $\Omega_0 = 1$  and  $\Omega_\Lambda = 0$ , a spectral index  $n = 1$ , a Hubble constant (in units of  $100 \text{ km s}^{-1} \text{ Mpc}^{-1}$ )  $h = 0.5$  and a baryon fraction  $\Omega_b = 0.0125h^{-2}$ , as predicted by the standard theory of the big bang nucleosynthesis — is not able to reproduce the clustering properties of the galaxy and cluster distribution and the cluster abundances, when normalized to the COBE data. As a consequence, a number of variants on this basic scenario have been suggested which might remedy its shortcomings. In this paper we consider different cosmological models which might be viable alternatives to the SCDM model; they all have a similar basic shape of power spectrum to SCDM but are engineered to have a smaller amount of small-scale power, which is the main problem with SCDM itself. In a general way, the initial (linear regime) power spectrum for all these models can be represented by

$$P_{\text{lin}}(k, 0) = P_0 k^n T^2(k), \quad (26)$$

where we use the fitting formula of the CDM transfer function as given by Bardeen et al. (1986):

$$T(k) = \frac{\ln(1 + 2.34q)}{2.34q} \left[ 1 + 3.89q + (16.1q)^2 + (5.46q)^3 + (6.71q)^4 \right]^{-1/4}. \quad (27)$$

In the previous equation  $q \equiv (k/h \text{ Mpc}^{-1})/\Gamma$ . The shape parameter  $\Gamma$  is related to the matter density parameter  $\Omega_{0m}$  and to the baryonic fraction  $\Omega_{0b}$  by the relation  $\Gamma = \Omega_{0m} h \exp[-\Omega_{0b} - \sqrt{h/0.5} \Omega_{0b}/\Omega_{0m}]$  (Sugiyama 1995).

**Table 1.** The parameters of the cosmological models. Column 2: the present matter density parameter  $\Omega_{0m}$ ; Column 3: the present cosmological constant contribution to the density  $\Omega_{0\Lambda}$ ; Column 4: the primordial spectral index  $n$ ; Column 5: the Hubble parameter  $h$ ; Column 6: the present baryon density  $\Omega_{0b}$ ; Column 7: the shape parameter  $\Gamma$ ; Column 8: the spectrum normalization  $\sigma_8$ ; Column 9: the non-linear value of the r.m.s. fluctuation amplitude inside a sphere of  $8h^{-1}$  Mpc  $\sigma_8^{nl}$ .

Model	$\Omega_{0m}$	$\Omega_{0\Lambda}$	$n$	$h$	$\Omega_{0b}$	$\Gamma$	$\sigma_8$	$\sigma_8^{nl}$
SCDM	1.0	0.0	1.0	0.50	0.050	0.45	1.22	1.16
SCDM <sub>CL</sub>	1.0	0.0	1.0	0.50	0.050	0.45	0.52	0.51
TCDM	1.0	0.0	0.8	0.50	0.100	0.41	0.72	0.72
TCDM <sub>GW</sub>	1.0	0.0	0.8	0.50	0.100	0.41	0.51	0.51
OCDM	0.4	0.0	1.0	0.65	0.036	0.23	0.64	0.66
$\Lambda$ CDM	0.4	0.6	1.0	0.65	0.036	0.23	1.07	1.13

To fix the amplitude of the power spectrum, we either attempt to fit the present-day cluster abundance or the level of fluctuations observed by COBE. For the latter, we parametrise the normalisation of the 4-year COBE data in terms of  $\sigma_8$ , the r.m.s. fluctuation amplitude inside a sphere of  $8h^{-1}$  Mpc, using the results of Bunn & White (1997), who used a Karhunen-Loève expansion to produce an unbiased estimate of the normalization, with a statistical uncertainty reduced to 7 per cent.

We will consider the following specific models, the main parameters of which are described in Table 1:

- the SCDM model, as reference model, with a normalization consistent with the COBE data;
- a different version of the SCDM model, hereafter called SCDM<sub>CL</sub>, with a reduced normalization corresponding to  $\sigma_8 = 0.52$  which produces a cluster abundance in better agreement with the observational data (Eke, Cole & Frenk 1996; see also Viana & Liddle 1996);
- a tilted model (hereafter TCDM; see e.g. Lucchin & Matarrese 1985; Vittorio, Matarrese & Lucchin 1988) with  $n = 0.8$  and high baryonic content ( $\Omega_{0b} = 0.1$ ; see White et al. 1996; Gheller, Pantano & Moscardini 1997);
- a different version of the previous model, hereafter TCDM<sub>GW</sub>, with a reduced normalization of the scalar perturbations ( $S$ ) that takes into account the possible production of gravitational waves (tensor perturbations  $T$ ) to the COBE fluctuations [we adopt the ratio  $T/S = 7(1-n)$  for the ratio of tensor to scalar contribution to the quadrupole, as predicted by some inflationary theories (e.g. Lucchin, Matarrese & Mollerach 1992; Lidsey & Coles 1992)];
- a open CDM model, with  $\Omega_{0t} = \Omega_{0m} = 0.4$ , COBE-normalized (hereafter OCDM);
- a low-density CDM model ( $\Omega_{0m} = 0.4$ ), with flatness provided by the cosmological term, i.e.  $\Omega_{0t} = 1$  and  $\Omega_{0\Lambda} = 1 - \Omega_{0m}$ , COBE-normalized (hereafter  $\Lambda$ CDM).

### 3 MODELLING THE BIAS OF GALAXIES

Though the number of ingredients is large in the models introduced above, the theoretical understanding of how clustering of matter grows via gravitational instability in the expanding Universe is quite well developed. As a consequence, it is relatively straightforward to compute the autocovariance function of matter fluctuations as a function of redshift in these scenarios. As we mentioned in Section 2.2, however, this does not lead us directly to a prediction of galaxy correlation properties because we still do not fully understand the details of the relationship between the whereabouts of the galaxies and the whereabouts of the mass. In principle, this relationship could be highly complicated, non-linear and environment-dependent. If this turns out to be the case then it is going to be very difficult indeed ever to unravel galaxy clustering observations to obtain information about the evolution of matter fluctuations and the cosmological parameters on which they depend. In this spirit, we are motivated to assume the relatively simple form of local bias represented by equation (2), though we do admit at the outset that things could be much more complex than this.

Having settled on equation (2), our task is now to determine the behaviour of the function  $b(M, z)$  for a given theoretical picture. In Paper I, we introduced four different general ideas of how different classes of cosmic objects might be related to the mass distribution and parametrised them in terms of the simplified biasing model we adopted. In this paper, we shall stick to the same four basic models, but adapt them to the specific situation of galaxy clustering.

The simplest biasing model one can imagine, and which is regarded by many as the most realistic, is described by  $b(M, z) = 1$ . This is called the *unbiased* model, though one has to be a little careful in using this terminology and motivation for it, particularly at high redshifts, is actually quite limited. In fact, it is not a trivial question to ask what is the formal definition of an unbiased population of objects, since one is attempting to relate two different types of

mathematical field: a point set and a continuous density field. One useful definition is that the population of objects constitutes a random (Poisson) sampling of the matter distribution, such as is the case if galaxies are selected by their luminosity which, in turn, is drawn from a universal (position-independent) luminosity function. But as galaxy formation occurs, stellar populations and luminosities evolve and galaxies undergo merging and tidal disruption, it is difficult to see how  $b(M, z)$  can be equal to unity for all properties  $M$  and redshifts  $z$ . In particular, at sufficiently high  $z$  one reaches the point where the first galaxy to form in the observable universe produced its stars. It clearly makes no sense to describe this object by an unbiased model in the sense we have used it here, even if one does not invoke density-dependent luminosity functions or other environmental effects. So even though it is very simple and, at least at first sight, self-consistent, we do not believe this model to be well motivated in the context of this paper so we use it here as a reference for the more complex models which follow.

An alternative picture of biasing can be constructed by imagining that galaxy formation occurs, for a given class of galaxies, at a relatively well-defined redshift  $z_f$ . (One can either assume that there is a single typical formation redshift for a certain class of galaxies or that there is some spread in it.) If this is the case, one can further imagine that galaxies which are born at a given epoch  $z_f$  might well be imprinted with a particular value of  $b(M, z_f)$ , in the spirit of equation (2), as long as the formation event is relatively local. If galaxies are biased by birth in this way, then they will not continue with the same biasing factor for all time, but will tend to be dragged around by the surrounding density fluctuations, which are perhaps populated by objects with a smaller bias parameter. In this case, the evolution of the bias factor can be obtained from (Dekel 1986; Dekel & Rees 1987; Nusser & Davis 1994; Fry 1996)

$$b(z) = 1 + (b_f - 1) \frac{D_+(z_f)}{D_+(z)}, \quad z < z_f, \quad (28)$$

where  $b_f$  is the bias at the formation redshift  $z_f$ ; we have suppressed the dependence on  $M$  here for brevity. This was called *galaxy-conserving model* in Paper I. Again, it is difficult to motivate this model in detail because it is difficult to believe that all galaxies survive intact from their birth to the present epoch, but it at least gives a plausible indication of the sense in which one expects  $b$  to evolve if the timescale for galaxy formation is relatively short and the timescale under which merging or disruption occurs is relatively long.

In most fashionable models of structure formation, however, the growth of large-scale features is driven by the hierarchical merging of sub-units. In these theories, one would not expect the survival of galaxies in their pristine initial state as anticipated in the galaxy-conserving model. Since the development of the clustering hierarchy is driven by gravity, the first things one has to understand are the properties of galactic haloes rather than the galaxies residing in them. One begins by calculating the bias parameter  $b(M, z)$  for haloes of mass  $M$  and ‘formation redshift’  $z_f$  at redshift  $z \leq z_f$  in a given cosmological model. The result is

$$b(M, z|z_f) = 1 + \frac{D_+(z_f)}{\delta_c D_+(z)} \left( \frac{\delta_c^2}{\sigma_M^2 D_+(z_f)^2} - 1 \right), \quad (29)$$

where  $\sigma_M^2$  is the linear mass-variance averaged over the scale  $M$  extrapolated to the present time ( $z = 0$ ) and  $\delta_c$  is the critical linear overdensity for spherical collapse [ $\delta_c = \text{const} = 1.686$  in the Einstein–de Sitter case, while it depends slightly on  $z$  for more general cosmologies (Lilje 1992)]. The above expression for the bias parameter was originally calculated by Mo & White (1996), although for simplicity they only gave results for  $z = 0$ . The general non-linear relation between the halo and the mass density contrast has been recently obtained by Catelan et al. (1997), by solving the continuity equation for dark matter haloes. Bagla (1997b) has discussed the clustering of haloes using numerical experiments. See also Ogawa, Roukema & Yamashita (1997) for a related discussion.

At this point one has to make some assumptions on how the galaxy is connected to the hosting halo and on what happens when the halo merges with other haloes. This point has been discussed at some length in the literature (e.g. Kauffmann, Nusser & Steinmetz 1997; Roukema et al. 1997) and many issues still remain unresolved: it is one of the most complicated aspects of galaxy formation. In order to make progress we shall simply assume in what follows that, however star formation and stellar evolution proceeds in a halo once it has formed, the properties of the resulting galaxy are in a one-to-one relationship with the parent halo mass  $M$ . Using this assumption it now becomes clear that we can drop the general interpretation of  $M$  in equation (3), as all properties of the galaxy are reducible to the parent halo mass (though see the comments in the last paragraph of this section).

Equation (3) is not the end of the story, however, because it does not tell us anything about what happens to the haloes after they have formed and, in particular, says nothing about the timescale of any merging. In the standard treatment of hierarchical clustering – the Press–Schechter (1974) theory – *all* the haloes that exist at a given stage merge immediately to form higher mass haloes, so that in practice at each time the only haloes which exist at all are those which just formed at that time. If one identifies the galaxies with their hosting haloes, then automatically  $z_f = z$  in the previous formula, i.e. the galaxy merging rate is automatically assumed to be much faster than the

**Table 2.** The best-fit parameters of the relation for the effective bias (30) computed for different minimum mass and different cosmological models.

	<i>SCDM</i>		<i>SCDM<sub>CL</sub></i>		<i>TCDM</i>		<i>TCDM<sub>GW</sub></i>		<i>OCDM</i>		<i><math>\Lambda</math>CDM</i>	
$M_{\min}$	$b_{\text{eff}}(0)$	$\beta$	$b_{\text{eff}}(0)$	$\beta$	$b_{\text{eff}}(0)$	$\beta$	$b_{\text{eff}}(0)$	$\beta$	$b_{\text{eff}}(0)$	$\beta$	$b_{\text{eff}}(0)$	$\beta$
$10^9 h^{-1} M_{\odot}$	0.42	1.97	0.48	1.94	0.48	1.97	0.56	1.95	0.51	1.96	0.44	1.98
$10^{10} h^{-1} M_{\odot}$	0.43	1.93	0.54	1.89	0.53	1.93	0.64	1.91	0.57	1.93	0.47	1.95
$10^{11} h^{-1} M_{\odot}$	0.46	1.86	0.66	1.82	0.61	1.87	0.80	1.86	0.69	1.87	0.51	1.90
$10^{12} h^{-1} M_{\odot}$	0.52	1.75	0.92	1.75	0.80	1.79	1.13	1.80	0.93	1.80	0.61	1.82
$10^{13} h^{-1} M_{\odot}$	0.69	1.64	1.56	1.73	1.21	1.74	1.85	1.77	1.47	1.75	0.84	1.73
$10^{14} h^{-1} M_{\odot}$	1.15	1.62	3.33	1.79	2.25	1.75	3.72	1.81	2.77	1.76	1.40	1.70

cosmological expansion rate. This is at the basis of what in Paper I we called the *merging model*. Of course this instantaneous-merging assumption is physically unrealistic and is related to the fact that one is using a mass variable which is continuous, while the aggregates of matter that form are discrete. On the other hand, it does provide a reasonable counter to the galaxy-conserving model introduced above.

In between these two extreme models one could assume that galaxies neither survive forever nor merge instantaneously. The price for this greater generality is that one requires an additional parameter to be introduced compared to equation (28). To understand how this intermediate model is constructed, it is easiest to look at how  $b(M, z)$  is used to calculate the quantity which is really required for observational comparisons, that is  $b_{\text{eff}}(z)$ , which appears in equation (1). Basically, one takes the ‘monochromatic’ (i.e. single mass) bias at each redshift (possibly with some extra parametric dependence on  $z_f$  different from  $z$ ) and then averages this monochromatic bias over the mass distribution of objects to obtain the ‘effective bias’, as described in equation (3). The latter quantity is to be used to connect the underlying mass autocorrelation function with the objects two-point function, which also requires convolution with the redshift distribution  $\mathcal{N}(z)$ ; see equation 1.

As in Paper I, we can estimate the effective bias by assuming that the objects observed in a given survey represent all haloes exceeding a certain cutoff mass  $M_{\min}$  at any particular redshift. In other words, we assume that there is a selection function  $\phi(z, M) = \Theta(M - M_{\min})$  at any  $z$ , where  $\Theta(\cdot)$  is the Heaviside step function. This is consistent with the reasoning we mentioned above, that all galaxy properties are reducible to the parent halo mass  $M$ . In this way, by modelling the linear bias at redshift  $z$  for haloes of mass  $M$  as in equation (29) and by weighting it with the theoretical mass-function  $\bar{n}(z, M)$  which we can self-consistently calculate using the Press–Schechter theory, we can obtain the behaviour of  $b_{\text{eff}}(z)$  directly. The results for different cosmological models are shown by the solid lines in Fig. 1, where various choices of the minimum cutoff mass in  $\bar{n}(z, M)$  are shown for reference.

The behaviour of  $b_{\text{eff}}(z)$  can be fitted by a relation of the form

$$b_{\text{eff}}(z) = 1 - 1/\delta_c + [b_{\text{eff}}(0) - 1 + 1/\delta_c]/D_+(z)^\beta. \quad (30)$$

The resulting best-fit parameters  $b_{\text{eff}}(0)$  and  $\beta$  are reported in Table 2 for different choices of initial matter fluctuation spectrum and minimum mass. In all cases, the effective bias is a increasing function of both redshift and  $M_{\min}$ . Notice further that a relatively strong anti-bias  $b_{\text{eff}} < 1$  can be produced at  $z = 0$  if the minimum mass is small, because all the small haloes still existing at a late stage of the clustering hierarchy will tend not to lie in dense regions.

So far this argument works equally well for the calculation of  $b_{\text{eff}}(z)$  in the framework of the merging model. But notice that the parameters of that model are entirely fixed because one has to match the evolution of the clustering hierarchy to observations at the present epoch. This amounts to matching the present-day value of  $b(z)$  by relating clustering properties of bright galaxies (e.g. the measured value of  $\sigma_8$  for these galaxies) to the analogous quantity predicted in a given model for the matter distribution. In terms of the argument given in the preceding paragraph, this basically means that  $M_{\min}$ , the free parameter, is fixed by requiring the present population of galaxies to have been entirely produced by a merger-driven hierarchy. On the other hand, we might decide that galaxies one might happen to see at large redshifts cannot be identified with the ancestors of present-day galaxies. In this case one can regard  $M_{\min}$  as a free parameter, but once a minimum mass is chosen, the value of  $b_{\text{eff}}$  implied at redshift  $z = 0$  will probably not correspond to the value of the bias parameter measured for any known class of objects. One must then assume that such objects are missing in local surveys, either because they had undergone a transient increase in their luminosity and have now faded or because they correspond to extended objects of low surface brightness, visible at high redshift, but invisible at small distances, due to selection effects. In Paper I we called this model the *transient model* and we will adopt this nomenclature here. To some extent this model is motivated most strongly for QSOs rather the galaxies (e.g. La Franca, Andreani & Cristiani 1997). Indeed, in the former context one can use efficiency



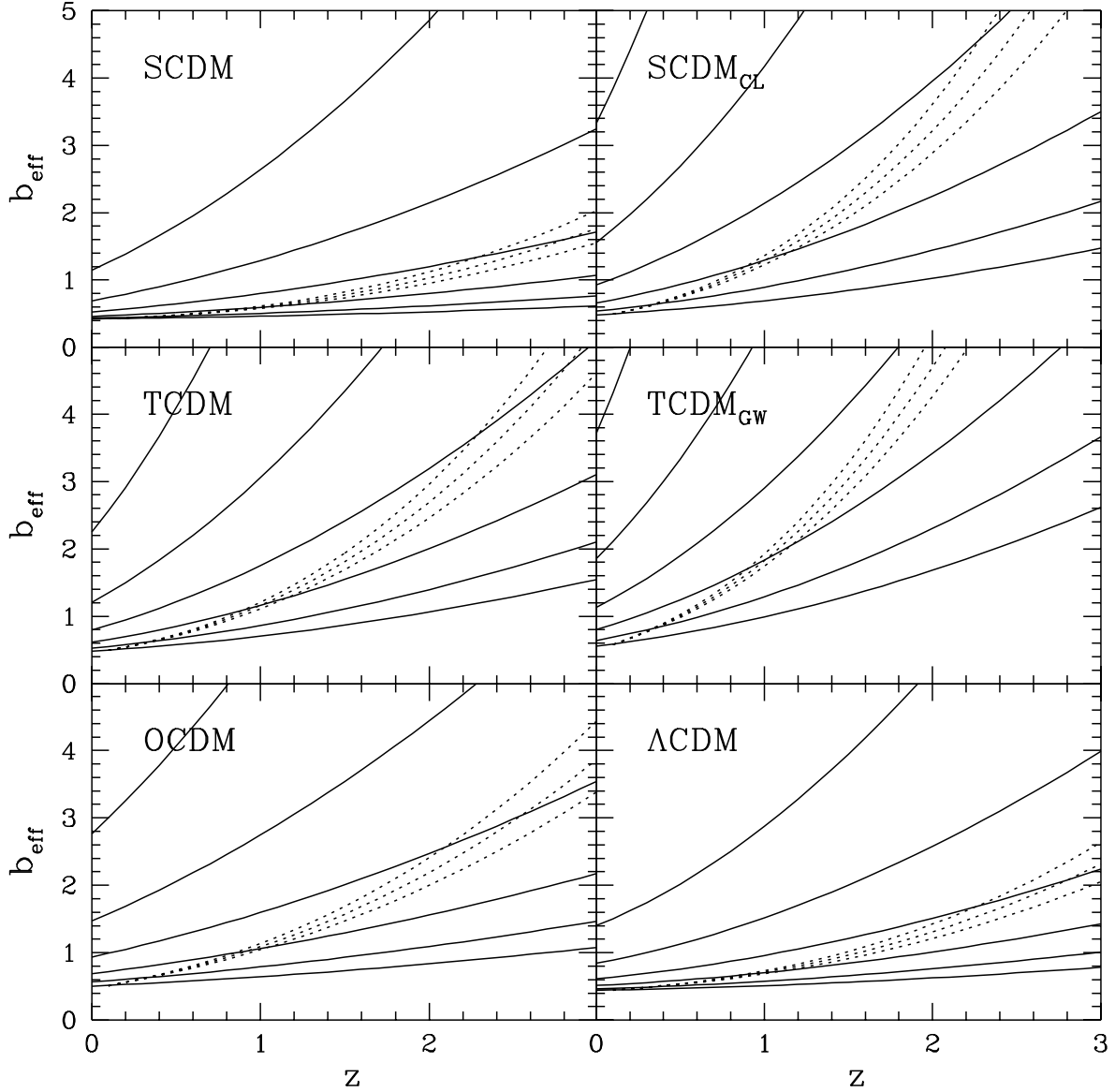


**Figure 1.** The effective bias  $b_{\text{eff}}$  as a function of the redshift  $z$  for the cosmological models considered in this paper. The different solid lines refer to different values of the minimum mass  $M_{\text{min}}$  in the Press-Schechter mass-function, ranging from  $10^9$  to  $10^{14} h^{-1} M_{\odot}$ , from bottom to top. The dotted lines show the effects of the catalogue selection: the results are obtained by assuming a bolometric magnitude limit  $m_{\text{lim}} = 24$ , a mass-to-luminosity ratio  $M/L = 10 M_{\odot}/L_{\odot}$  and a K+E-correction expressed by the relation  $\mathcal{K} \log(1+z)$ , with  $\mathcal{K} = -1, 0, +1$  (from bottom to top).

arguments proposed by Efstathiou & Rees (1988) to obtain a relatively high minimum halo mass in that case. In the galactic setting the choice of halo mass is less obvious, and may be much smaller than those which host QSOs, which may be as large as  $\sim 10^{12} M_{\odot}$ .

We should make the point that these simple schemes do not exhaust all the possible scenarios through which galaxies might have formed and evolved. For example, it is quite possible that merging could play a different role at different redshifts. Present day bright disk galaxies, for example, have clearly not just formed at the present epoch since their properties suggest a lack of mergers in the recent past. On the other hand, it is plausible that galaxies at much higher redshifts, say  $z \sim 2$ , are undergoing merging on the same timescale as the parent haloes. This suggests the possible applicability of a model where rapid merging works at high redshift, but it ceases to dominate at lower redshifts and the bias then evolves by equation (28) until now. In this context it is interesting to note that, while  $b_f$

is a free parameter in equation (28), it is actually predicted by equation (30), once the appropriate minimum mass is specified. Thus matching the merging phase (30) onto the conserving phase (28) gives

$$b_f = 1 + (b_0 - 1)D_+^{-1}(z_f) = 1 - \frac{1}{\delta_c} + \left(b_{\text{eff}}^*(0) - 1 + \frac{1}{\delta_c}\right) D_+(z_f)^{-\beta} \quad (31)$$

for the bias these objects would have at  $z_f$  when they stopped merging. In this equation  $b_{\text{eff}}^*(0)$  is to be interpreted as the effective bias the galaxies would have now if they continued merging from  $z_f$  until now; since the galaxies do not do this, the actual present-day bias will be different. Evolving from  $z = z_f$  until  $z = 0$  using equation (28) yields

$$b_0 = 1 - \frac{D_+(z_f)}{\delta_c} + \left(b_{\text{eff}}^*(0) - 1 + \frac{1}{\delta_c}\right) D_+^{1-\beta}(z_f). \quad (32)$$

It is interesting to speculate whether the clustering of present-day ‘bright’ galaxies can be explained in this picture. For example, in an Einstein-de Sitter model, such galaxies must have  $b_0 \simeq 2$  if the constraint on  $\sigma_8$  from cluster abundances is correct (Eke, Cole & Frenk 1996; Viana & Liddle 1996), since  $\sigma_8$  measured for these objects is of order of unity. In order to obtain  $b_0 \simeq 2$ , we need to have the last term in equation (32) to be of order unity. Unless  $z_f$  is very large, this means a relatively large value of  $b_{\text{eff}}^*(0)$  which, from Table 2, requires a relatively large minimum mass of order  $10^{12} h^{-1} M_\odot$  for those models with  $\sigma_8 \simeq 0.5$ . Such a picture would therefore explain a large present-day value of the bias of galaxies with very large haloes, if these galaxies could be identified with objects that for some reason had not undergone significant merging in the recent past. Whether this interpretation is consistent with observations of the dependence of galaxy merger rates with redshift (e.g. Ellis 1997; Neufschaefer et al. 1997; Roche, Eales & Hippelein 1997) is a subject for further study. Notice that in open models and models with non-vanishing cosmological constant the value of  $\sigma_8$  coming from the constraint on the cluster abundance is larger (see e.g. Viana & Liddle 1996). For example, for  $\Omega_{0m} = 0.4$ ,  $\sigma_8 \simeq 0.8$  is required. Consequently the present-day ‘bright’ galaxies must have  $b_0 \simeq 1.3$  and the corresponding minimum mass can be smaller. We shall not investigate this model any further in this paper, however, as it contains nothing that makes it qualitatively different from the previous examples.

We can now summarize these arguments by introducing a simple unified model for bias which incorporates all four of these previous examples as special cases. As noticed in Paper I, all these models can be described by the equation

$$b_{\text{eff}}(z) = b_{-1} + (b_0 - b_{-1})/D_+(z)^\beta, \quad (33)$$

with suitable parameters  $b_0$ ,  $b_{-1}$  and  $\beta$ ;  $b_{-1}$  may be interpreted as the bias factor at the end of the era of cosmological expansion, i.e. at the maximum expansion in a closed model, or as  $t \rightarrow \infty$  in an open or flat model. The particular examples we consider are:

- the unbiased model, with  $b(z) = 1$ ;
- the transient model, where the parameters are fixed by the choice of the minimum mass (see Table 2); we will use  $M_{\text{min}} = 10^{11} h^{-1} M_\odot$ ;
- the merging model, where the parameters are fixed by the value of the bias parameter at  $z = 0$  ( $b_0 = 1/\sigma_8$ ) and taking the bias relation for the corresponding minimum mass;
- the galaxy-conserving model, which has  $b_{-1} = \beta = 1$  and  $b_0 = 1/\sigma_8$ .

In order to be fully consistent with our formalism, we adopt the non-linear value of the r.m.s. fluctuation amplitude inside a sphere of  $8h^{-1}$  Mpc,  $\sigma_8^{nl}$ , computed by using the PD96 method. The values of  $\sigma_8^{nl}$  for the different cosmological models are reported in the last column of Table 1.

In Fig. 2, we display the actual evolution of  $b_{\text{eff}}(z)$  for each of the cosmologies and for each of these four biasing models. Notice that there is a considerable variation in the behaviour expected depending on the cosmology under consideration, except (of course) for the unbiased model. We shall return to this in the next Section.

As final point, we should mention how the bias factor changes when catalogue selection effects are considered, i.e. when theoretical quantities, as the mass  $M$ , are substituted with the observational ones, such as the luminosity  $L$ . After choosing one of the models above, one will end up with the quantity  $b(M, z)$  to be understood as ‘the bias that objects of mass  $M$  have at redshift  $z$ ’. The effective bias at the same redshift is precisely

$$b_{\text{eff}}(z) = N(z)^{-1} \int d \ln L \Phi_{\text{obs}}(L) b[M(L), z], \quad (34)$$

where  $N(z) = \int d \ln L \Phi_{\text{obs}}(L)$  and  $\Phi_{\text{obs}}(L)$  is the *observed* luminosity function of the catalogue, i.e. the intrinsic luminosity function multiplied by the catalogue selection function, which will typically involve a cut in apparent magnitude in whatever wave-band is being used, rather than in the somewhat idealised case we discussed above where everything corresponds to a cut in mass  $M$ . Because of this cut (for magnitude or flux-limited catalogues), in order to obtain  $b_{\text{eff}}$  one should need to know the distance modulus of the galaxies at a given  $z$ , including all

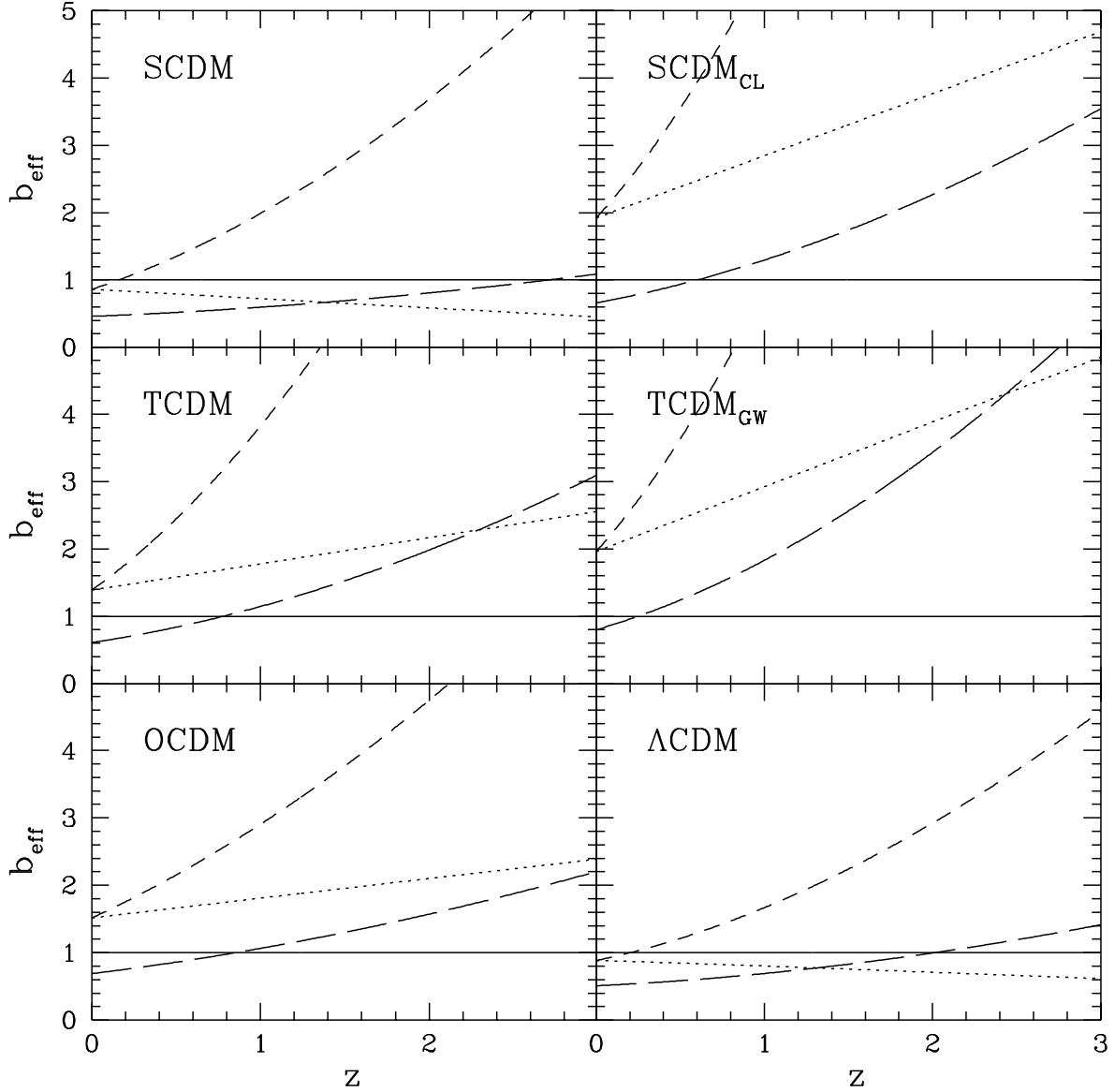


**Figure 2.** The fits to the function  $b_{\text{eff}}(z)$  for each cosmology discussed in this paper and for the four different biasing models described in the text: unbiased model (solid line); galaxy-conserving model (dotted line); merging model (short-dashed line); transient model (long-dashed line).

possible K-corrections and evolutionary (E) effects in order to calculate this exactly. Furthermore, because the bias is typically expressed as a function of mass, one needs to know the mass-to-light ratio in the given wave-band. To test the size of this effect we computed an illustrative example for all the cosmological models described above, assuming a bolometric magnitude limit of  $m_{\text{lim}} = 24$ , a mass-to-luminosity ratio  $M/L = 10 M_{\odot}/L_{\odot}$  and a K+E-correction parametrised by the relation  $\mathcal{K} \log(1+z)$ . The results for  $\mathcal{K} = -1, 0, +1$  are shown as dotted lines in Fig. 1. The general effect of this ‘selection bias’ is to exaggerate the increase of the bias factor with redshift even further. This is particularly evident when small minimum masses  $M_{\text{min}}$  are considered, though it has little effect on the quantitative results we have obtained in the next section, and none at all on their qualitative interpretation. We shall not therefore discuss this detail any further in our analysis.

#### 4 SIMPLE MODELS OF CLUSTERING EVOLUTION

As we mentioned in the Introduction, theoretical interpretations of information on clustering evolution have frequently been rather naive. In particular, many observational results are quoted in terms of the parameter  $\epsilon$  in the following simple scaling model for the redshift evolution of the two-point correlation function  $\xi(r, z)$  at the comoving separation  $r$ :

$$\xi(r, z) = \xi(r/(1+z), 0)(1+z)^{-(3+\epsilon)}. \quad (35)$$

If the spatial dependence of the two-point function can be fitted by a power-law with slope  $\gamma$ , the above relation further simplifies to

$$\xi(r, z) = (r/r_c)^{-\gamma}(1+z)^{-(3-\gamma+\epsilon)}, \quad (36)$$

where  $r_c$  is a constant measuring the unit crossing of  $\xi$  at  $z = 0$ .

Recent observational studies (e.g. Le Fèvre et al. 1996; Shepherd et al. 1997; Carlberg et al. 1997; Roche, Eales & Hippelein 1997; Woods & Fahlman 1997) have served to highlight the importance of understanding the validity (or otherwise) of the simple models (35) & (36). It is still commonplace for observational data to be framed in terms of  $\epsilon$  as if this parameter had some unambiguous theoretical significance. For example, Le Fèvre et al. (1996) and Shepherd et al. (1997) have reported a value of  $\epsilon \sim 1 \pm 1$  from an analysis of galaxy clustering at moderate redshifts. But what does this imply for theoretical models?

Assuming that clustering grows by gravitational instability alone, the above formulae can be interpreted in a few special cases. For  $\epsilon = 0$  it reproduces the prediction of the so-called *stable clustering* model (cf. Peebles 1980), while for  $\epsilon = n + 2 = \gamma - 1$ , it results from the application of linear theory in an Einstein–de Sitter universe to purely scale-free power spectra with  $P_{\text{lin}}(k, 0) \propto k^n$ . The case where  $\epsilon = \gamma - 3$  corresponds to a clustering pattern that simply expands with the background cosmology as if the galaxies were just painted on a homogeneous background.

Concerning the case of stable clustering ( $\epsilon = 0$ ), one should remember that the idea underlying the stable clustering ansatz is that, on sufficiently small scales, gravity acts to stabilize the number of neighbours of an object in a proper volume, after this has turned around from the universal expansion. Numerical simulations, however, suggest that this type of dynamical regime is only entered, if at all, when the mass autocorrelation function is at least as large as  $\sim 100$  (e.g. Efstathiou et al. 1988; Bagla & Padmanabhan 1996; Padmanabhan 1996; Munshi & Padmanabhan 1997; Jain 1997; Munshi et al. 1997), which only occurs on scales much smaller than the dimensions of typical surveys. Melott (1992) considered the growth of clustering in numerical simulations for an ensemble of scale-free models. He found that the lower the value of the spectral index  $n$ , the larger is the value of the parameter  $\alpha \equiv 3 - \gamma + \epsilon$  and that positive values of  $\epsilon$  are easily allowed for in all models with  $n \leq 1$ . Melott's explanation for such a fast clustering growth is as follows: stable clustering is not an upper limit to the growth of correlations; whenever the initial conditions contain non-vanishing large-scale power, merging makes new clusters form and their central density increases with time, which in turn enhances the growth of correlations. Moreover, a numerical study of the evolution of the two-point function both for the matter and halo population has been carried out by Colín, Carlberg & Couchman (1997); they obtain a scale-dependent  $\epsilon$  parameter which is about 1 for mass particles in an Einstein–de Sitter universe, and lower for low-density models. A broad range of values (ranging from  $-0.2$  to  $1$  in the flat case and reaching lower values in the open case) is obtained for haloes, depending on their mean density (see also Brainerd & Villumsen 1994). Jain (1997) has discussed the reliability of the general relation of equation (35) in the context of various models. His conclusions are that the above parametrisation for the evolution of clustering is inaccurate in CDM-like models, for two reasons. First, because the growth of  $\xi(r, z)$  with time on intermediate scales is much faster than the  $(1+z)^{-3}$  law prescribed by stable clustering at fixed proper separation (see also PD96) and, second, because the boundary between the linear, mildly non-linear and stable clustering regimes, occurs at scales which rapidly change with time.

As one can therefore see, the theoretical interpretation of  $\epsilon$  is open to some doubt. This doubt widens when one considers the different ways  $\epsilon$  could be defined when the correlation function is not of power-law type and the dynamical evolution is not of the self-similar form, situations which are actually expected in realistic models. In this case one could define  $\epsilon$  to be the value at a particular proper or comoving distance  $r$  where the slope  $\gamma$  can be defined, perhaps the scale corresponding to  $r_0$ . Alternatively, one could fit a power-law to all the data and use this to define  $\gamma$  and get  $\epsilon$  that way. In general these values of  $\epsilon$  will not be equal. Likewise,  $\epsilon$  at a given scale  $r$  need not be constant with time (or redshift).

To illustrate the problem we have calculated, in Fig. 3, the behaviour of  $\epsilon$  (defined at two fixed proper separations corresponding to  $1h^{-1}$  Mpc and to the value of  $r_0$  at the present epoch) for three of our models (SCDM<sub>CL</sub>, OCDM,  $\Lambda$ CDM); cf. Mo (1997). The value of  $\epsilon$  at  $z$  is obtained by fitting the correlation function  $\xi$  in the redshift interval  $[0, z]$ . The results for the mass (solid line) are relatively constant with redshift. Notice that for this case the value of

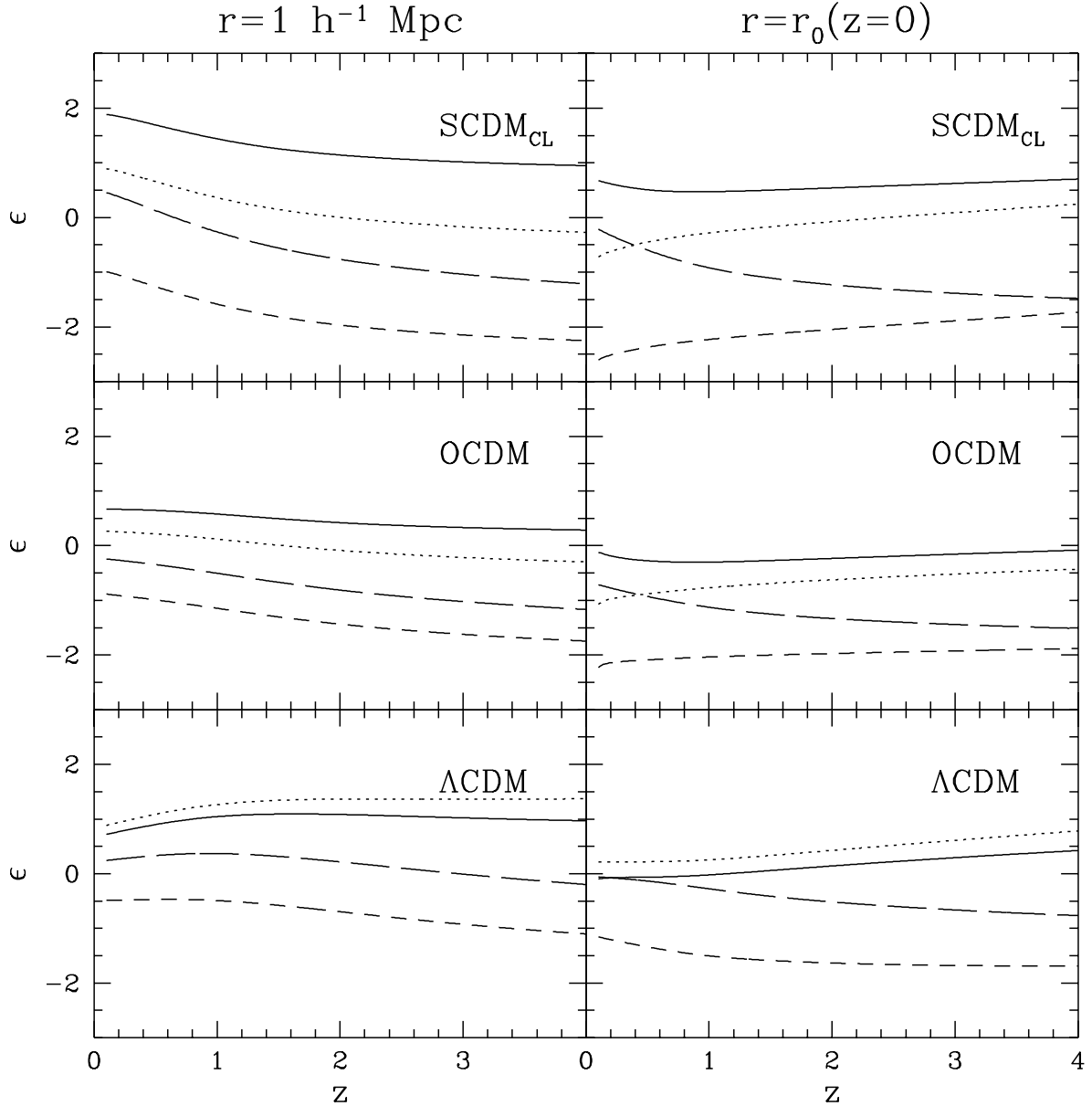


**Figure 3.** The behaviour of the scaling parameter  $\epsilon$  measured at a fixed physical length scale (equal to  $1h^{-1}$  Mpc on the left and equal to the present correlation length  $r_0$  on the right) for models with three different background cosmologies. Different biasing models are as Fig. 2.

$\epsilon$  is higher than the stable clustering value, probably due to the effects of merging. But in any case the scale probed here is much larger than the scale at which one expects stable clustering to apply in a flat Universe. In the open case, the matter distribution actually matches  $\epsilon = 0$  quite closely, which is expected because bound objects suffer no future disturbance in open models when free expansion takes over (cf. Padmanabhan et al. 1996). The  $\Lambda$ CDM model is intermediate between these two, with clustering only freezing out much later as the expansion begins to accelerate.

The situation for the *galaxies*, however, is much more confused than the case for the matter. Different biasing models yield very different predicted behaviours for  $\epsilon(z)$ , which suggests that the usefulness of this parametrisation of clustering is most limited for precisely those objects which one could actually observe. Notice also that the value of  $\epsilon$  depends on the scale at which it is measured, adding further confusion to its interpretation.

As well as  $\epsilon$ , which measures the rate of evolution, one is also interested in what the characteristic length scale of clustering might be as a function of redshift. One way to encode this information is via the quantity  $r_0(z)$ , the

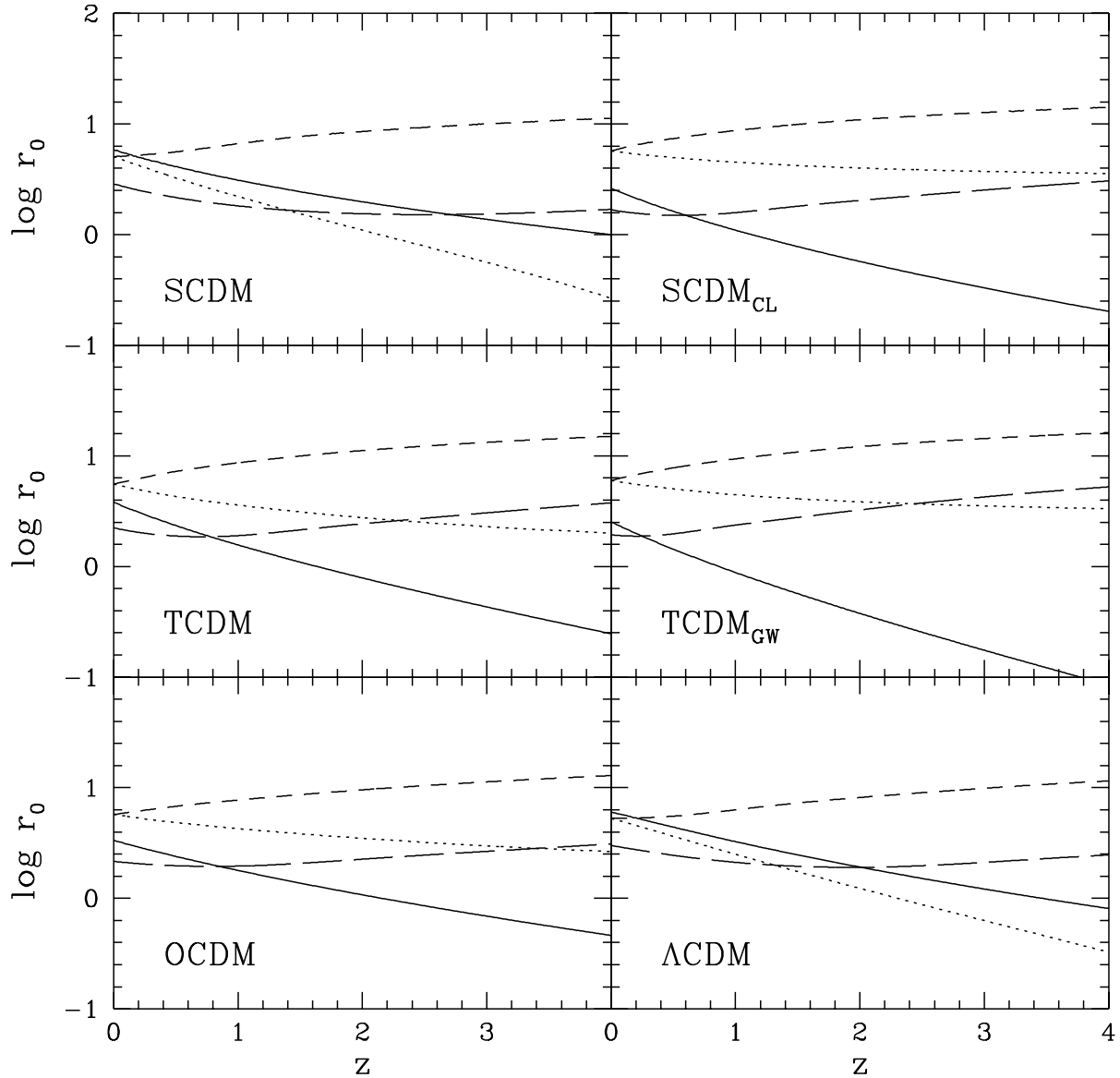


**Figure 4.** The behaviour of the (comoving) correlation length  $r_0$  (in units of  $h^{-1}$  Mpc) as a function of redshift for the various models considered. Different biasing models are as in Fig. 2. Note that, although the matter correlation length always decreases in comoving coordinates, the correlation function of galaxies need not do so if there is significant and evolving bias.

distance at which the correlation function has unit amplitude. This quantity represents a kind of characteristic scale of the clustering pattern, so one might try to compare the sizes of individual structures with this quantity.

In hierarchical clustering models, the generic expectation is that this (comoving) characteristic scale must decrease with increasing redshift. Fig. 4 demonstrates that, while this is certainly true for the distribution of mass, it need not be true for galaxies selected with particular forms of bias. An  $r_0$  that increases with redshift is obtained in both merging and transient models in most cases.

The fundamental point that arises from these considerations concerns the approach one adopts to test theories. In the present situation, one is attempting to eliminate some particular well-defined models from a shortlist of contenders. In other words, our aim is hypothesis testing. This kind of test is best performed in the ‘observational plane’, i.e. by computing exactly what an observer would see in a given model universe and comparing it with what is seen in ours. It is not useful in our view to treat the problem as one of inference, where one tries to fit a model parameter (in this case  $\epsilon$ ) to the observations, particularly a parameter which is of such limited usefulness and theoretical significance.

## 5 APPLICATIONS AND RESULTS

### 5.1 The surveys

In the following subsections we will apply our formalism to the correlation analyses (both angular and projected) of four different datasets, recently constructed for the study of the distribution of high-redshift galaxies.

The Canada–France Redshift Survey (CFRS; Le Fèvre et al. 1996 and references therein) consists of 591 galaxies with certain spectroscopic redshifts and magnitudes in the range  $15.5 \leq I_{AB} \leq 22.5$ . The sample covers 71 square arcminutes. The redshift distribution (Crampton et al. 1995) extends up to  $z \sim 1.6$  with more than 60 per cent of galaxies with redshift larger than  $z = 0.5$ .

The Hawaii Keck K-band sample used in the study of Carlberg et al. (1997) is an almost complete sample up to  $K = 20$ ,  $I = 23$  and  $B = 24.5$  magnitudes covering an area of about 27 square arcminutes. The redshift distribution, presented in Carlberg et al. (1997), is slightly changed with respect to an earlier version of that paper, used in Paper I. Now it contains 248 galaxies, the 80 per cent of them with redshifts between  $z = 0.28$  and  $z = 1.39$ .

The Hubble Deep Field (HDF) is a program of very deep observations made from the Hubble Space Telescope in four passbands and covering a field at high galactic latitude. Different galaxy catalogues have been extracted from the HDF (Williams et al. 1996; Clements & Couch 1996). In their analysis, Villumsen, Freudling & da Costa (1997) use a total of 1732 galaxies detected in the F606W filter which has characteristics similar to an R passband. Recently estimates of the redshift distribution based on photometric redshifts have been obtained by different authors (Mobasher et al. 1996; Sawicki, Lin & Yee 1997; Connolly et al. 1997). In order to compare our predictions with the Villumsen, Freudling & da Costa (1997) results, we are forced to use the same redshift distribution adopted in that paper, i.e.

$$\mathcal{N}(z) = 2.723 \frac{z^2}{z_0^3} \exp[-(z/z_0)^{2.5}] , \quad (37)$$

where  $z_0$  is the median redshift.

The last dataset here considered is the survey for  $z \sim 3$  galaxies recently started by Steidel et al. (1996, 1997). Their observations use the  $U_n$ ,  $G$  and  $R$  photometric system that is sensitive to the Lyman break in high-redshift objects. After spectroscopic confirmation, they found 67 objects with redshift  $z > 2$  in one of their fields (SSA22a+b), covering an angular area of  $8.74' \times 17.64'$ .

### 5.2 The CFRS angular correlation function

In Fig. 5 we show the model predictions for the angular correlations of the CFRS catalogue limited to  $z < 1.6$ . In the same plot we also show the observational results obtained by Hudon & Lilly (1996) using two different methods which likely bracket the true values: local and global determinations are presented by open and filled squares, respectively.

Notice that for SCDM, only the merging model is compatible with the data, indicating that one cannot reconcile the objects in this survey with observed galaxies at low redshift. All other biasing models fail to reproduce the data within the SCDM framework: the predicted evolution of clustering is too strong in this scenario. In the other cosmological models, the transient model is always compatible with the data, and for some of them (SCDM<sub>CL</sub>, TCDM, TCDM<sub>GW</sub> and OCDM) also the unbiased model can roughly reproduce the data. The data are incompatible with both the merging and galaxy-conserving models for any cosmology.

### 5.3 Keck K-band angular correlation function

Carlberg et al. (1997) computed the angular correlation function for the Keck dataset limited to  $z < 1.6$ . The comparison between these results and our various models is shown in Fig. 6.

The rather large errors on the observational correlations mean that discriminatory power is less than in the previous case. Basically, all biasing schemes are compatible with the data in any of the models, although the merging model predictions are uncomfortably high for both versions of SCDM and TCDM.

### 5.4 Hubble Deep Field Angular Correlations

Villumsen, Freudling & da Costa (1997) computed the two-point angular correlation function for the HDF survey using eight different magnitude limits, ranging from  $R = 26$  to  $R = 29.5$ . Here we prefer to compare the predictions of our different models to the observational results only for the catalogue with limit  $R = 29$ , corresponding to a median redshift  $z_0 = 1.87$  in equation (37). With this choice the observational results have the smaller errorbars and are expected to be more discriminant. In fact, the results, shown in Fig. 7, impose impressively strong constraints on

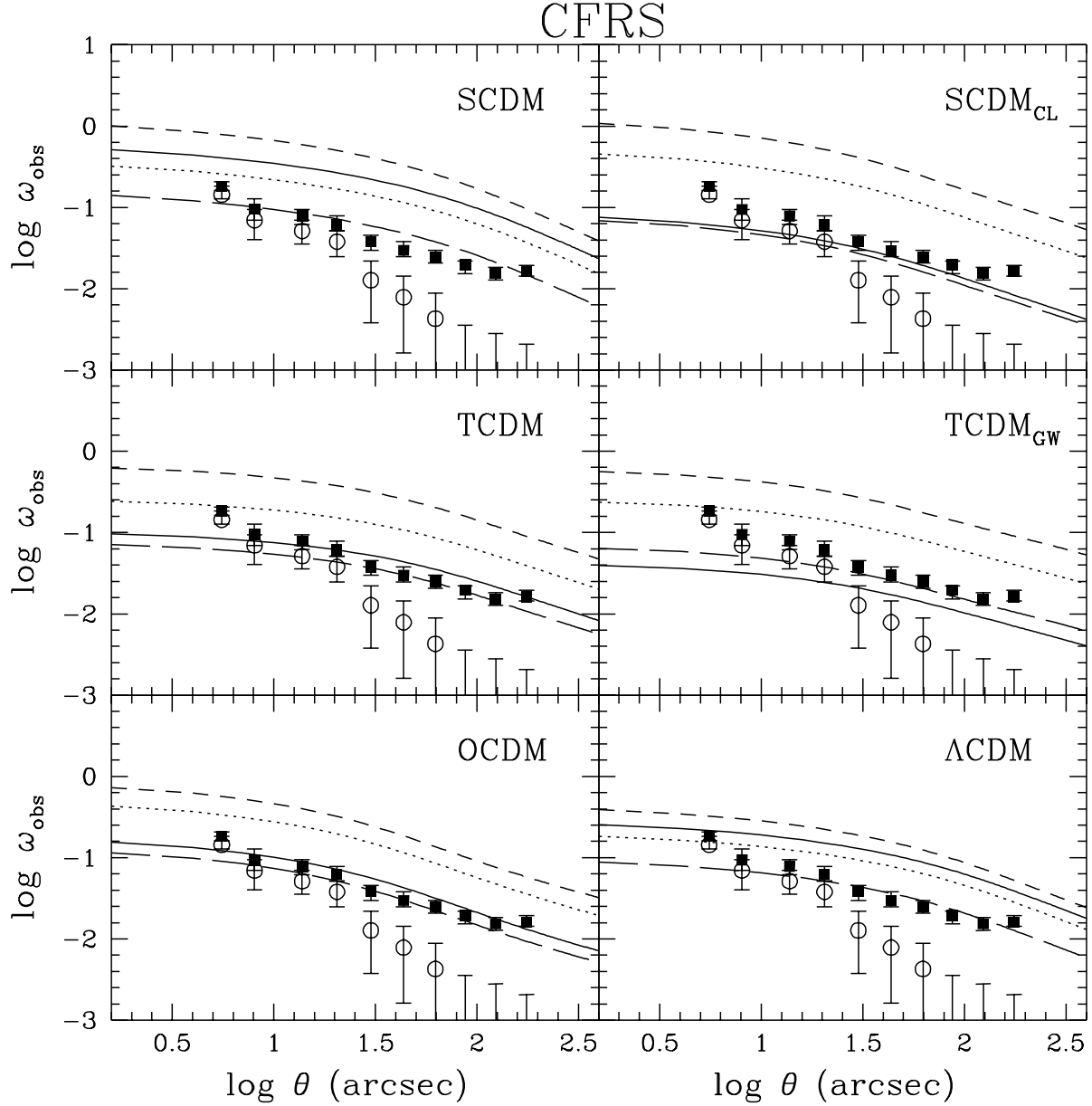


**Figure 5.** Theoretical prediction in different cosmological models for the angular galaxy correlation function from the Canada–France Redshift Survey. The galaxies have  $z < 1.6$  and  $\mathcal{N}(z)$  is taken from Crampton et al. (1995). Correlation data are from Hudon & Lilly (1996) and are obtained by using two different methods which bracket the true values: the local and global determinations are shown by open circles and filled squares, respectively. Different bias models are considered, as in Fig. 2.

the combination of biasing scheme and cosmological model. *All* combinations are excluded for SCDM. The merging model is always excluded in any cosmology. The galaxy-conserving model can fit the data only within the  $\Lambda$ CDM model. The models which appear to be in best agreement with the data are the unbiased and transient bias schemes in low density models (either with or without a  $\Lambda$ -term).

### 5.5 CFRS Projected Correlation Function

The CFRS data have been analysed also in terms of the projected correlation function by Le Fèvre et al. (1996). They divided the galaxies in three different strips in redshift with median redshift  $z \approx 0.34$ ,  $z \approx 0.62$  and  $z \approx 0.86$ . We use these median redshifts to rescale in comoving coordinates the projected separations, originally plotted in proper coordinates. Their correlations have been computed by using  $q_0 = 0.5$ ; consequently the results have to be translated



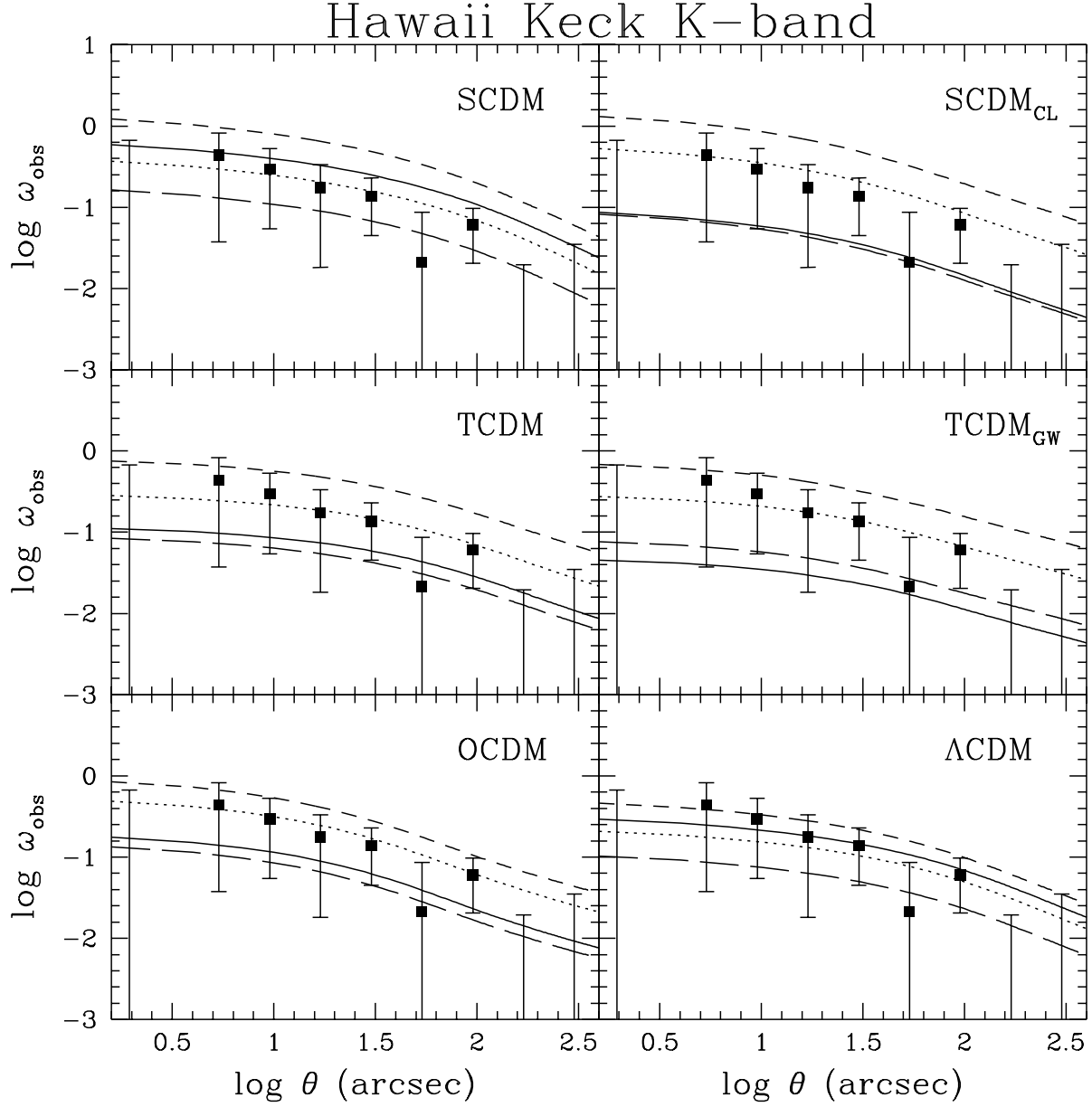


**Figure 6.** Theoretical prediction in different cosmological models for the angular galaxy correlation function from the Hawaii K-band Survey. The galaxies are in the redshift range  $0 < z < 1.6$ , with redshift distribution and correlation data taken from Carlberg et al. (1997). The original data are corrected to take into account the dilution produced by the uncorrelated foreground stars. Different bias models are shown as in Fig. 2.

for different models because both  $w(r_p)$  and the distance  $r$  depend on cosmology. For this goal we follow Peacock (1997a), particularly his discussion of the same observational dataset in Section 4.1 of that paper and specifically using his equation (40).

The results, presented in Fig. 8, show that the transient model is compatible with the data for all cosmologies, though this is marginal in the case of SCDM. The unbiased model is compatible with the data for SCDM<sub>CL</sub>, TCDM and OCDM. On the other hand, the merging and galaxy-conserving models are always inconsistent.

## 5.6 Keck K-band Projected Correlation Function

The projected correlation function has been computed also for the Hawaii Keck K-band survey by Carlberg et al. (1997). They present the results for four different redshift strips, with median redshift  $z \approx 0.34$ ,  $z \approx 0.62$ ,  $z \approx 0.97$

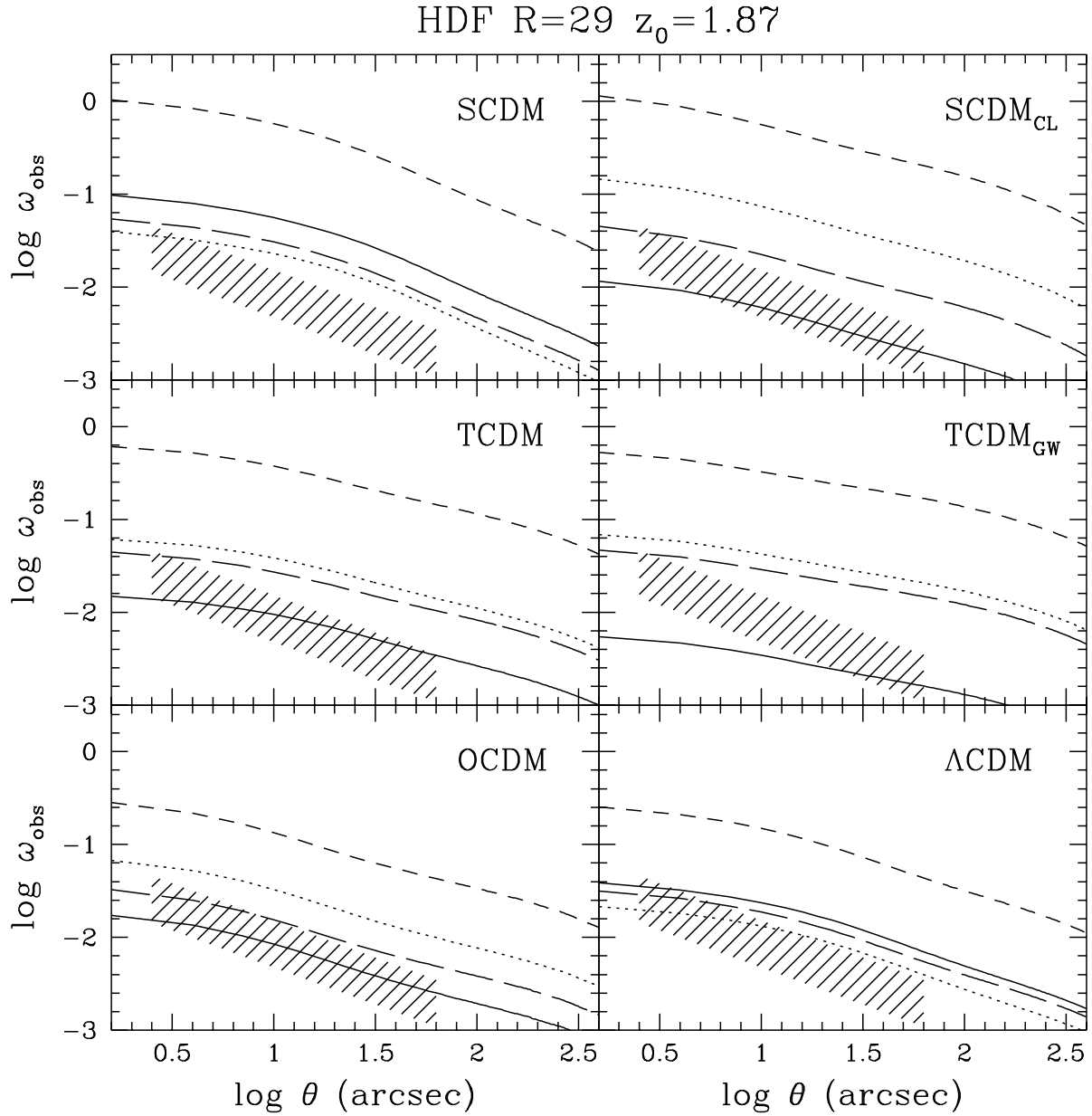


**Figure 7.** Theoretical prediction in different cosmological models for the angular galaxy correlation function for the Hubble Deep Field. The results are for the sample with magnitude limit  $R = 29$  and median redshift  $z_0 = 1.87$ . The redshift distribution is given by equation (37). The shaded region in the plots refers to the  $1\sigma$  range allowed by the fit obtained on the observational data by Villumsen, Freudling & da Costa (1997). Different bias models are shown as in Fig. 2.

and  $z \approx 1.39$ , by adopting  $q_0 = 0.1$ . As before, we rescale in comoving coordinates by using the median redshifts and we translate the observational results for different cosmological models following Peacock (1997a). Notice that the observational data used here are different with respect to those used in Paper I presented in an earlier version of the Carlberg et al. paper.

Interpretation of the results, reported in Fig. 9, is slightly complicated by the strange shape of the measured correlation function at low  $z$ . One could resort to a scale-dependent bias to solve this difficulty (see below), but in any case this makes it difficult to exclude models on the basis of the results for the low redshift bin. It is worthwhile, however, considering what one might conclude if some of these results were subject to an unknown error. If one accepts the points at small separations as being ‘accurate’, then they favour the number-conserving and merging models in all the cosmologies, and also are consistent with an unbiased model for  $\Lambda$ CDM and SCDM. If instead one

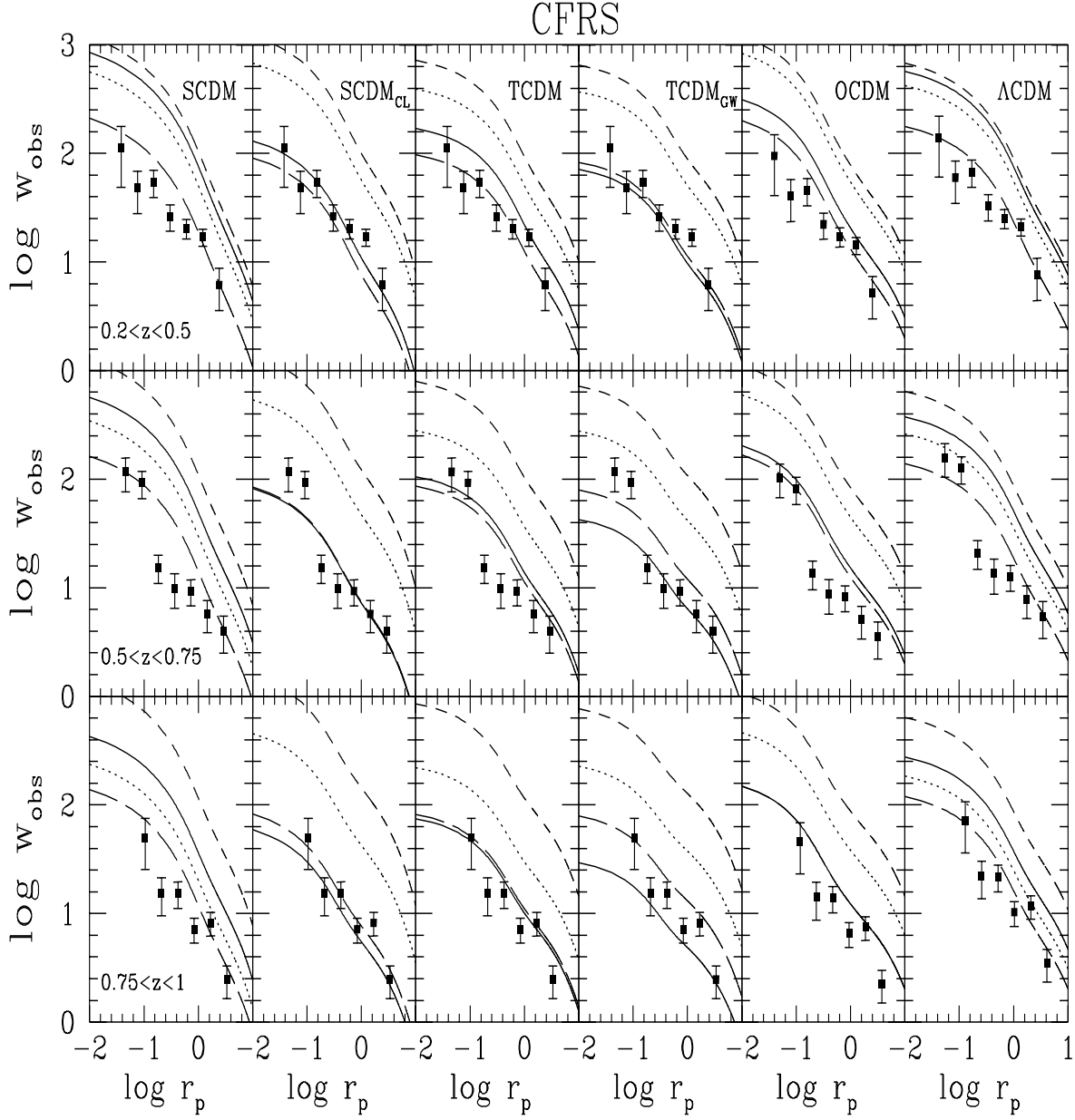


**Figure 8.** Theoretical prediction in different cosmological models for the projected galaxy correlation function of the Canada–France Redshift Survey sample as a function of the (comoving) separation  $r_p$  (in units of  $h^{-1}$  Mpc). The redshift distribution is given by Crampton et al. (1995). Correlation data are from Le Fèvre et al. (1996). Different rows refer to different strips in redshift:  $0.2 < z < 0.5$  (top),  $0.5 < z < 0.75$  (centre) and  $0.75 < z < 1$  (bottom). Different bias models are shown as in Fig. 2.

discards these points and concentrates on the intermediate separation points, they favour the transient and unbiased models for SCDM, TCDM and OCDM.

The data at larger redshifts have much larger errors, but it emerges robustly that the merging model is excluded by the data for any cosmology. Generally speaking the unbiased and transient model are reasonable fits in all cases considered, though for SCDM the unbiased case is only marginally acceptable. For consistency, these results at higher  $z$  lead one to prefer the interpretation that the putative problem with the low-redshift data does indeed affect the small-separation points, rather than those at larger scale but this argument is, of course, not rigorous.

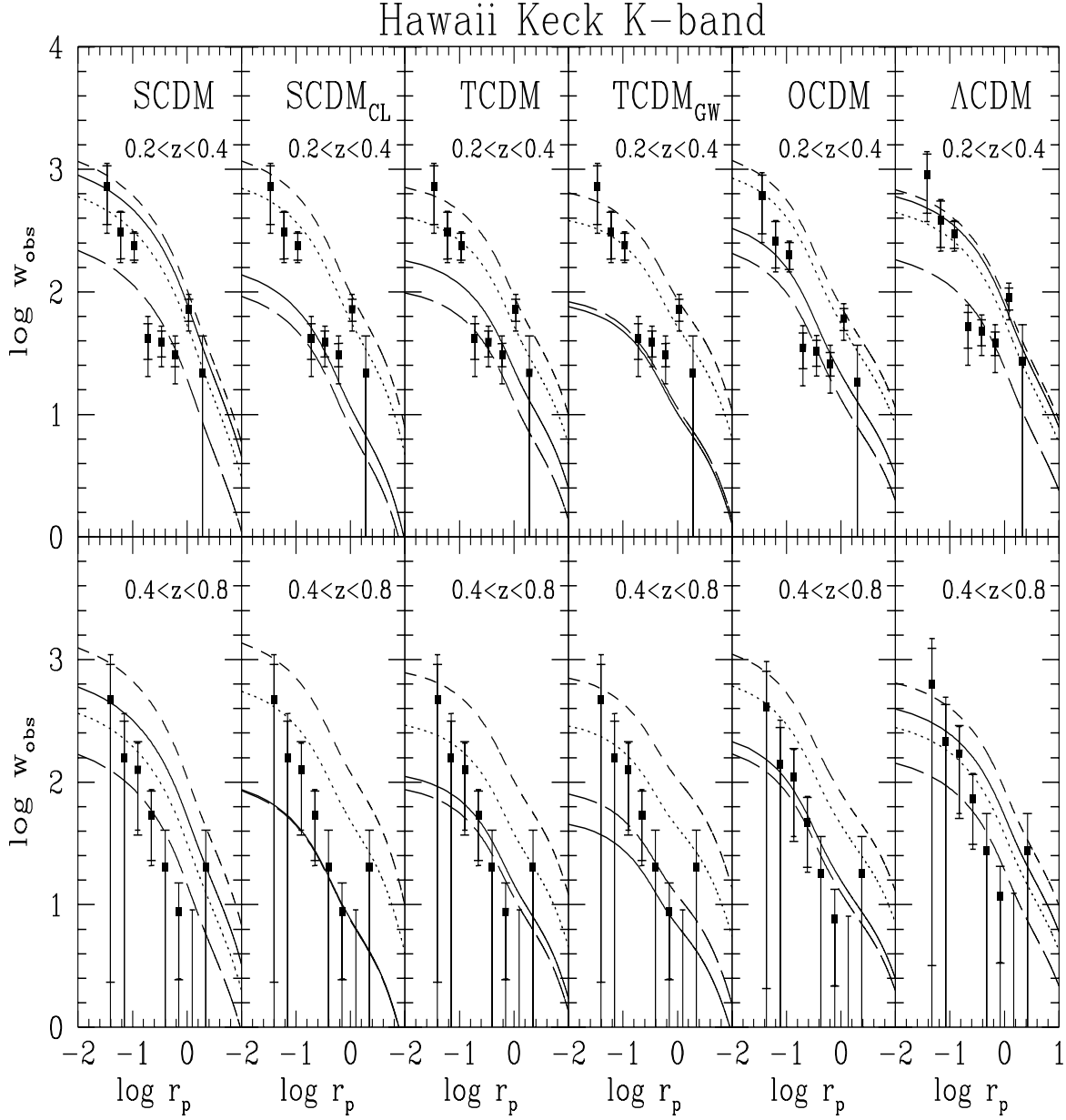


**Figure 9.** a. Theoretical prediction in different cosmological models for the projected galaxy correlation function of the Hawaii Keck K-band survey as a function of the (comoving) separation  $r_p$  (in units of  $h^{-1}$  Mpc). The redshift distribution and correlation data are from Carlberg et al. (1997). The  $1\sigma$  bootstrap and the poissonian errorbars are shown by narrow and wide error flags, respectively. Different rows refer to different strips in redshift:  $0.2 < z < 0.4$  (top) and  $0.4 < z < 0.8$  (bottom). Different bias models are shown as in Fig. 2.

### 5.7 Lyman-Break Galaxies

Steidel et al. (1996, 1997) have reported evidence for the existence of a strong concentration of galaxies at  $z \sim 3$  in their angular field. This ‘spike’ contains 15 objects (plus one faint QSO) in a redshift bin of width  $\Delta z = 0.04$ . Various authors have discussed the probability of such an object arising in particular cosmological scenarios (Mo & Fukugita 1996; Steidel et al. 1997; Baugh et al. 1997; Bagla 1997a; Jing & Suto 1997; Governato et al. 1997; Peacock 1997b; Wechsler et al. 1997), reaching somewhat equivocal conclusions.

Although not designed for this particular problem, which can only be resolved in an entirely satisfactory fashion using N-body simulations, the formalism we have constructed in this paper can be used to shed qualitative light on the concentration of Lyman-break galaxies in a very simple way. In principle, the correct theoretical tool to this

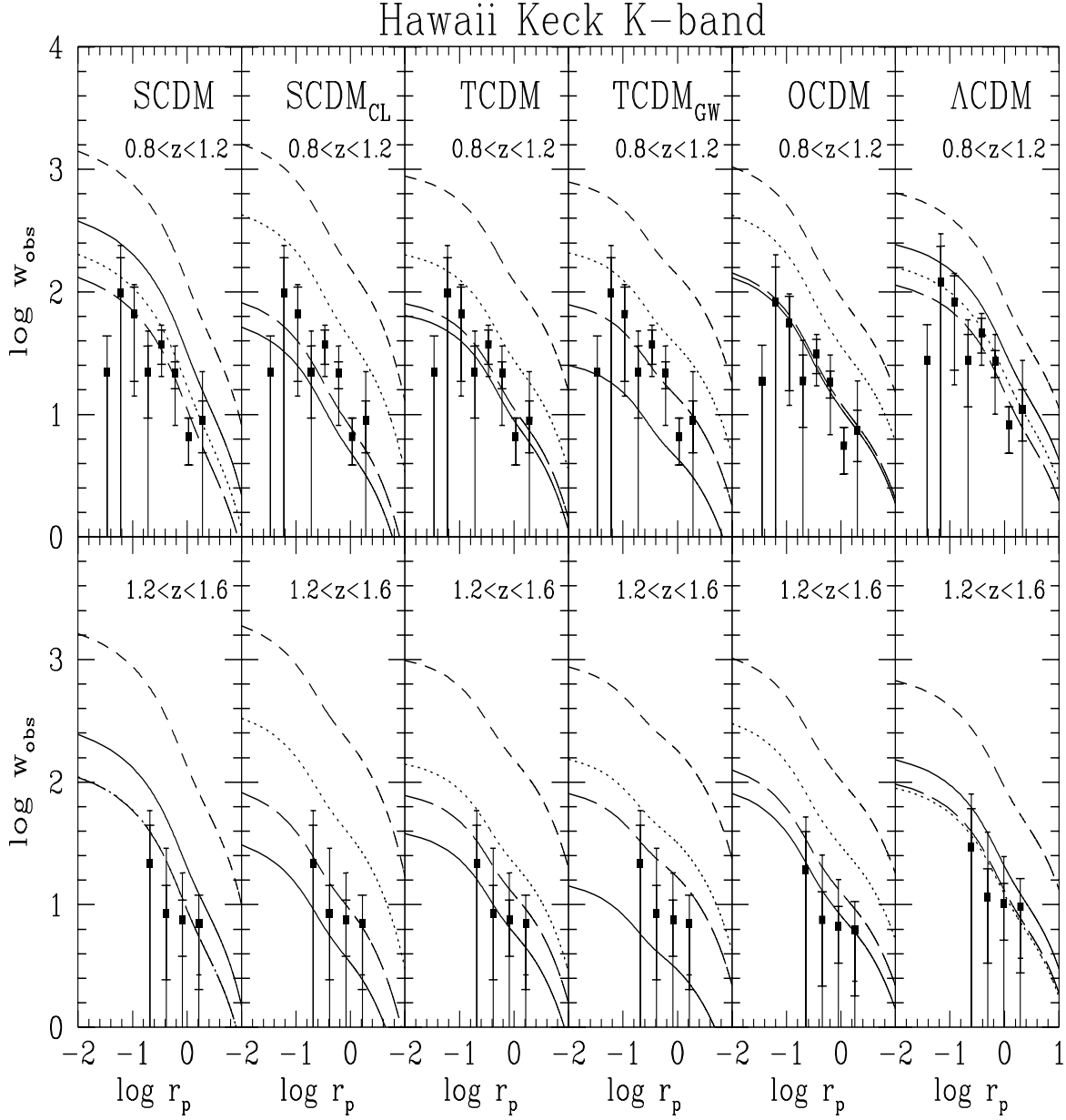


**Figure 9. b.** As Fig. 9a but for different strips in redshift:  $0.8 < z < 1.2$  (top) and  $1.2 < z < 1.6$  (bottom).

purpose would be the formula for the probability of finding  $N$  objects in a given volume, which for each model depends on both the mean number of objects and on all the hierarchy of correlation functions, suitably smoothed over the volume (White 1979). However, no sound theoretical predictions exist for the evolution of the entire hierarchy of correlation functions into the non-linear regime. We can, however, get a useful insight by calculating the expected number of neighbours  $N_R$  within a distance  $R$ , given the presence of an object at the origin. This is larger than the mean number of galaxies in a randomly-selected volume by factor of  $[1 + \bar{\xi}(R)]$ ; this factor therefore measures the average ‘excess’ number of galaxies that tend to accompany a given galaxy. At redshift  $z$ , the quantity  $N_R$  is related to the integrated mass correlation function  $\bar{\xi}$  by  $N_R = \bar{N}[1 + b_{\text{eff}}^2(z)\bar{\xi}(R, z)]$ , where  $\bar{N}$  is the mean number of objects in a sphere of radius  $R$ . In order to calculate this we need to know three different quantities: the value of  $\bar{N}$ ; the radius  $R$  corresponding to the volume of the considered bin; the appropriate model of bias.

The value of the mean number of objects can be taken directly from the smoothed redshift selection function, obtained by Steidel et al. (1997) from the whole survey. From their Fig. 1, it is possible to infer that  $\bar{N} \sim 4.5$  at  $z \sim 3$ . As for the radius  $R$ , the volume of the bin depends on the cosmology because of the dependence of proper

**Table 3.** The predictions of the expected number of Lyman-break galaxies inside a sphere of radius  $R = 7.5$ ,  $R = 10$  and  $R = 12.5 h^{-1}$  Mpc ( $N_{7.5}$ ,  $N_{10}$  and  $N_{12.5}$  respectively) for different cosmological models. Two different values for the minimum cutoff mass ( $M_{\min} = 10^{11}$  and  $10^{12} h^{-1} M_{\odot}$ ) are used. The values of the effective bias  $b_{\text{eff}}$  at redshift  $z = 3$  and the comoving correlation length  $r_0$  (in units of  $h^{-1}$  Mpc) are also reported.

	$M_{\min} = 10^{11} h^{-1} M_{\odot}$					$M_{\min} = 10^{12} h^{-1} M_{\odot}$				
	$b_{\text{eff}}(z = 3)$	$N_{7.5}$	$N_{10}$	$N_{12.5}$	$r_0$	$b_{\text{eff}}(z = 3)$	$N_{7.5}$	$N_{10}$	$N_{12.5}$	$r_0$
<i>SCDM</i>	1.07	5.2	4.9	4.8	1.5	1.72	6.4	5.6	5.2	2.7
<i>SCDM<sub>CL</sub></i>	3.50	6.0	5.4	5.0	2.5	6.38	9.5	7.4	6.3	4.9
<i>TCDM</i>	3.12	6.7	5.9	5.4	3.0	5.11	10.5	8.2	6.9	5.7
<i>TCDM<sub>GW</sub></i>	5.54	8.0	6.7	6.0	4.2	9.30	14.4	10.6	8.6	7.3
<i>OCDM</i>	2.18	6.3	5.7	5.3	2.6	3.55	9.4	7.6	6.7	5.0
<i><math>\Lambda</math>CDM</i>	1.43	6.0	5.4	5.1	2.1	2.24	8.1	6.8	6.1	4.1

distances on angles and redshift intervals. The translation of the angular size of the field and the width of the redshift bin into volumes therefore depends upon the parameters  $\Omega_m$  and  $\Omega_{\Lambda}$ . The bin is roughly equivalent to a sphere with  $R = 7.5 h^{-1}$  Mpc in a universe with  $\Omega_{0m} = 1$  and a factor  $\sim 1.5$  larger in the other cosmologies here considered. As thoroughly discussed by Steidel et al. (1997) and Bagla (1997a), redshift distortions can also be very important inside the bin. In particular, it seems quite likely (on the basis of its high redshift) that the concentration of Lyman-break galaxies is still collapsing. Collapse in the observer's line-of-sight would tend to enhance the concentration observed in redshift space relative to the real space concentration and meaning that the real space length scale of the structure should be larger than that perceived in redshift measurements. This argues for a larger value of  $R$  than the previous values. In order to allow for these uncertainties, in the following analysis we will consider, for all the models, three different values of  $R$ :  $R = 7.5$ ,  $R = 10$  and  $R = 12.5 h^{-1}$  Mpc. We will call the corresponding results  $N_{7.5}$ ,  $N_{10}$  and  $N_{12.5}$ , respectively.

The last problem is the choice of the bias model. As already discussed in Section 3, the process of merging is expected to dominate at high redshift, when structures are still forming hierarchically. In order to mimic the behaviour of the Lyman-break galaxies we can therefore reasonably assume the behaviour of  $b_{\text{eff}}$  shown in Fig. 1 (with the fits reported in Table 2). The results for two different values for the minimum cutoff mass ( $M_{\min} = 10^{11}$  and  $10^{12} h^{-1} M_{\odot}$ ) are reported in Table 3.

It is clear from Table 3 that, for all choices of the parameter  $M_{\min}$  and for all allowed values of  $R$ , the expected number is always smaller than the observed one. However, the mean number of objects in a randomly-selected bin at this redshift would be around 4.5. If the presence of one galaxy in the bin is imposed then this number rises to the number given in the table. If a typical fluctuation can raise the number from 4.5 to around 10, as it can for models with the higher minimum mass, then a number around 15 is certainly not an inconceivably large fluctuation. We would expect fluctuations about the mean excess to be at least of the same order as the mean itself. Only SCDM (and, more marginally,  $\Lambda$ CDM) seems to have some problems getting close to the value required, mainly due to the low value of the bias parameter. Obviously, the predicted numbers decrease when larger radii are considered, increasing the gap between model predictions and observations. Consequently, the effect on the final results of including redshift distortions can be very strong.

Another comment can be made on the minimum mass. In order to have better agreement with the Steidel et al. (1997) result,  $M_{\min}$  has to be of order  $10^{12} h^{-1} M_{\odot}$  or more. This seems to indicate that the Lyman-break galaxies should be interpreted as progenitors of massive galaxies at the present epoch (e.g. Steidel et al. 1997) or precursor of present day galaxy clusters (e.g. Governato et al. 1997).

Consistency of these Lyman-break galaxy data with the model predictions also requires that the mean number of objects estimated by Steidel et al. (1997) is generally smaller (because of selection effects) than the mean number of these objects predicted by the theory. This can be estimated in our formalism by using the Press-Schechter formula to get the number of haloes more massive than  $M_{\min}$  at redshift  $z \sim 3$ . We checked that all our models satisfy this constraint (see also Jing & Suto 1997), but predicting precisely which haloes give rise to a Lyman-break galaxy is beyond the scope of our theory.

Our formalism also allows to predict the spatial correlation function  $\xi_{\text{obs}}$  of the Lyman-break galaxies. To this aim we use equation (1), where the redshift distribution is taken from Steidel et al. (1997) and the bias models is chosen as before. The results obtained for a minimum mass of  $10^{12} h^{-1} M_{\odot}$  (that we found to be in better agreement with the observation of the concentration of 15 galaxies at  $z \sim 3$ ) are shown for the different cosmological models in Fig. 10. From their N-body simulations, Governato et al. (1997) found that the effect of redshift distortions is strong

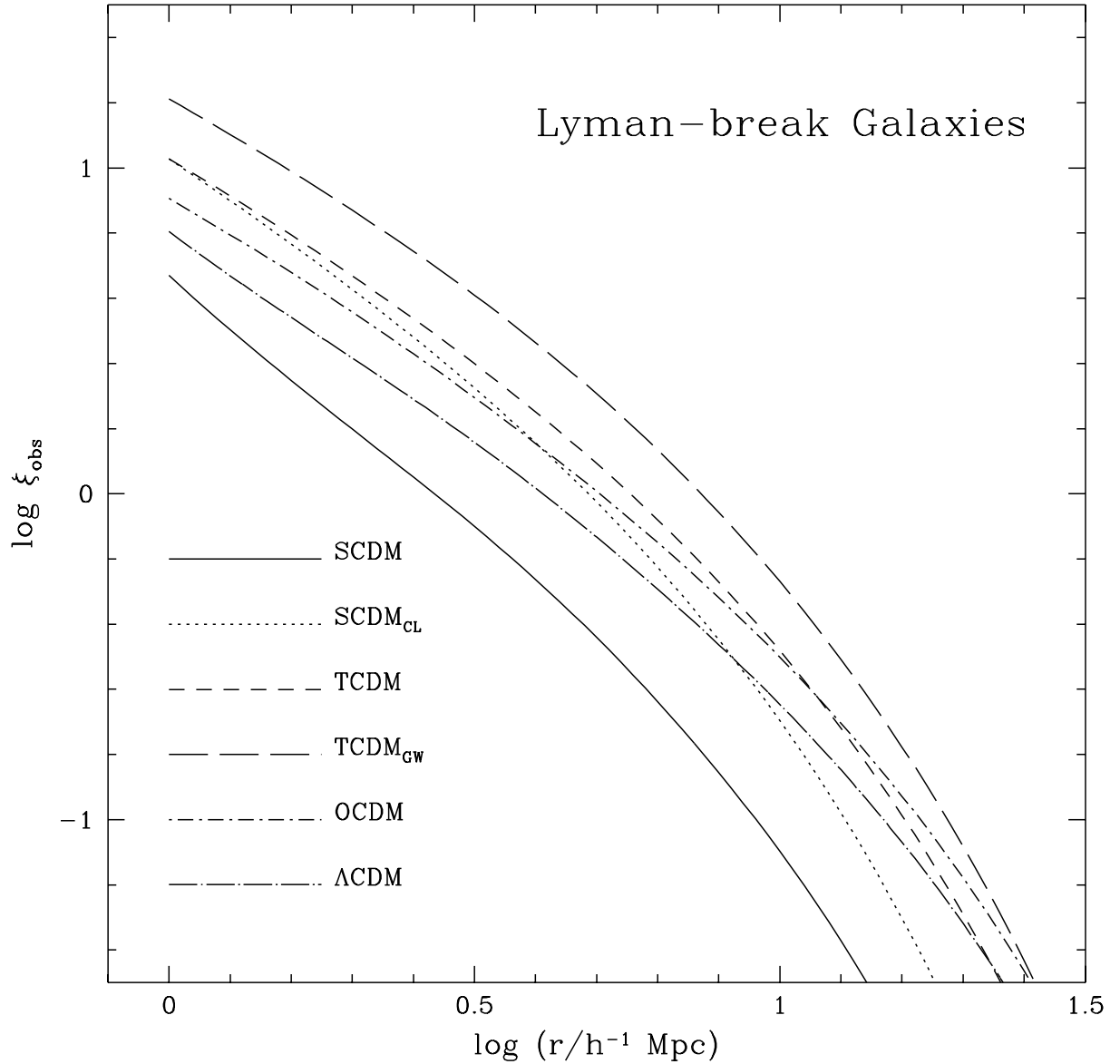


**Figure 10.** Theoretical prediction in different cosmological models for the observed spatial correlation function of the Lyman-break galaxies as a function of the (comoving) separation  $r$  (in units of  $h^{-1}$  Mpc). The redshift distribution is taken from Steidel et al. (1997). A minimum mass of  $10^{12}h^{-1}M_{\odot}$  is used to compute the effective bias.

at (comoving) scales smaller than  $\sim 1h^{-1}$  Mpc (see also Wechsler et al. 1997). For this reason we prefer to plot our results only for larger scales. We find that the predictions for the various models are quite different, in agreement with the analysis of Wechsler et al. (1997). The correlation length  $r_0$  (reported in Table 3) ranges from  $2.7h^{-1}$  Mpc for SCDM to  $7.3h^{-1}$  Mpc for TCDM<sub>GW</sub>. These differences, mainly due to the large spread in the value of the bias parameter  $b_{\text{eff}}$  at high redshifts, seem to indicate that the measurement of the correlation function of these objects (when reliably available) can be used to constrain the cosmological models.

### 5.8 General Comments

The problem posed by several of these data sets concerns the *slope* of the correlation function rather than its amplitude. One should not at this stage, however, infer very negative conclusions about cosmological structure formation scenarios on the basis of the shape. As we mentioned above, we have assumed that the bias is modelled by a constant bias

factor. As was shown by Coles (1993), this is not the generic expectation even in local bias models and, indeed, one expects to see a steepening of the correlation function on small scales resulting from the introduction of non-linear terms into a generic biasing relation of the form

$$\delta_n(\mathbf{x}; M, z) \simeq f_{M,z}[\delta_m(\mathbf{x}, z)] . \quad (38)$$

The more non-linear the function  $f$ , the steeper one expects the galaxy correlation function to be compared with the matter correlations. One also expects this phenomenon to be more prominent when the linear bias factor (which can be thought of as the first term in a series approximation to  $f$ ) is large, i.e. at high  $z$ . The observed correlation functions one sees do tend to be steeper than the theoretical predictions at small separations, especially in Fig. 9a, so this might well be connected with these effects and should not necessarily lead one to argue that none of the models we present is compatible with the data. It is also quite possible for the bias to be even more complicated than this. In particular, it may be of non-local form so that the propensity of a galaxy to form at a particular position depends not only on the density at that point, but on the density at surrounding points. Such a non-local bias may be induced by astrophysical effects resulting in some kind of feedback (e.g. Babul & White 1991; Bower et al. 1993). A non-local bias is also induced purely dynamically, because haloes remember the conditions at their Lagrangian birthplace (Catelan et al. 1997).

It is also worth mentioning the somewhat surprising fact that the differences in predictions of the cosmological models considered, while they are significant, are not perhaps as large as one would naively imagine. In particular, one might have expected the  $\Lambda$ CDM model and OCDM model to display the biggest differences because the linear growth law is so different in these cases. One can see, however, that when non-linear and bias evolution are incorporated, these models make predictions for most of the observational setups that are not drastically out of line with the other scenarios considered.

Finally, in this section we remind the reader that the correlation amplitudes measured by observers in our theoretical universes would be even larger than the quantities we have presented because of the effect of the amplification bias introduced by gravitational lensing. Since most of the failed models are excluded because they overpredict the strength of clustering anyway, this only reinforces our conclusions.

## 6 DISCUSSION AND CONCLUSIONS

In this paper we have explored a number of issues arising from the confrontation of observational evidence of high-redshift clustering against observations. We have stressed the importance of constructing exact statistical descriptions of clustering so that this confrontation can be carried out in an objective and accurate way. The calculation of the statistical quantities required to test particular models is not trivial because it demands the inclusion of a number of different effects but, as we have shown, this can be done when all relevant aspects are modelled systematically.

As in Paper I, we have stressed the crucial importance of understanding more clearly the relationship between galaxies and mass, and how this relationship evolves with cosmic epoch. Even the simplest plausible models of bias introduce large uncertainties into the clustering pattern predicted in different theories. We also emphasise that these biasing schemes are probably over-simplifications: the bias may well be non-local and/or scale-dependent and may involve significantly more astrophysics than we have included in our discussion. It is a first priority to understand much better the relationship between galaxies and the underlying matter distribution, particularly the relationship between galaxy properties and those of the parent haloes. Some progress is clearly being made in this area by the application of phenomenological models of hierarchical galaxy formation (e.g. Kauffmann, Nusser & Steinmetz 1997). Ultimately, however, the way forward will probably involve all-inclusive numerical simulations that can handle gravity, hydrodynamics and star formation simultaneously. On the other hand, it is reassuring that even the relatively small data sets available to us have allowed sizeable chunks of the parameter space of these models to be eliminated. In the meantime, we can be reasonably confident that further data will lead to stronger constraints on the simple models available at present.

We have compared some currently fashionable models of structure formation with the available observational data using the statistical tools mentioned in the previous paragraph. The present data have fairly large experimental errors, but do offer significant power to discriminate between models. This situation can only improve as more and better high-redshift data are accumulated. In particular we found Hubble Deep Field (HDF) data to be highly discriminatory. More data of this type, such as is anticipated from the proposed further deep surveys with HST, would be extremely useful.

The details of the comparison of observations with data are discussed in the previous Section, but it is worth emphasizing a few general inferences that can be drawn by taking all the results together. First, we can conclude that if the ‘correct’ model of large-scale structure is indeed one of those we have discussed here, then both the rapid merging



and galaxy-conserving models of galaxy formation are excluded by the data. The second point is that those cosmologies that can reproduce the observed abundance of rich clusters can also match the galaxy clustering observations, but only if galaxies are no more than moderately biased at redshifts of order unity. Since the models we are testing involved a complicated interplay of the various components (background cosmology, perturbation spectrum, biasing scheme, etc.) it is difficult to draw deeper conclusions from the data about any one of these components. In particular, one might have hoped that the rate of evolution of galaxy clustering might lead one more-or-less directly to the value of the density parameter,  $\Omega$ . Although the available data show no strong preference for either high or low values of  $\Omega$ , the  $\Lambda$ CDM model does seem to fit both amplitude and shape of the available marginally better than models with a higher density; this is particularly so at relatively low redshifts. On the other hand, the data do generally prefer a value of the bias parameter of order unity. A low value for the bias parameter of bright galaxies tends, on other grounds, to favour  $\Omega < 1$  (e.g. Peacock 1997a; Coles & Ellis 1997).

Finally, we stress that constraints emerging from clustering arguments, like those we have presented here, are significantly more robust than those based solely on number-densities, which are very sensitively dependent on assumptions about the halo parameters and galaxy formation efficiency. Quantities based on overdensities, such as  $\xi(r)$ , are constructed to be independent of the underlying number-density of objects and one can, at least in principle, use them to make reliable predictions even when the predicted number-density of objects is uncertain. For this reason, we expect many useful constraints on models to derive from ongoing and planned observational surveys.

## ACKNOWLEDGMENTS.

R.G. Carlberg and O. Le Fèvre are warmly thanked for providing us with electronic versions of their results. We are grateful to S. Arnouts for helpful discussions, to Y. Jing for useful comments about the Lyman-break galaxies and to John Peacock for clarifying for us the interpretation of the PD formalism at  $z \neq 0$ . LM thanks the QMWC for its hospitality. PC is grateful to the Dipartimento di Astronomia at the Università di Padova for hospitality during a visit. Italian MURST is acknowledged for partial financial support. PC is a PPARC Advanced Research Fellow.

## REFERENCES

- Babul A., White S.D.M., 1991, MNRAS, 253, 31  
 Bagla J.S., 1997a, MNRAS, in press, astro-ph/9709230  
 Bagla J.S., 1997b, preprint, astro-ph/9711081  
 Bagla J.S., Padmanabhan T., 1996, ApJ, 469, 470  
 Bardeen J.M., Bond J.R., Kaiser N., Szalay A.S., 1986, ApJ, 304, 15  
 Baugh C.M., Cole S., Frenk C.S., Lacey C.G., 1997, preprint, astro-ph/9703111  
 Bower R.C., Coles P., Frenk C.S., White S.D.M., 1993, ApJ, 405, 403  
 Brainerd T.G., Villumsen J.V., 1994, ApJ, 431, 477  
 Bunn E.F., White M., 1997, ApJ, 480, 6  
 Carlberg R.G., Cowie L.L., Songaila A., Hu E.M., 1997, ApJ, 484, 538  
 Carroll S.M., Press W.H., Turner E.L., 1992, ARA&A, 30, 499  
 Catelan P., Lucchin F., Matarrese S., Porciani C., 1997, preprint, astro-ph/9708067  
 Clements D.L., Couch W.J., 1996, MNRAS, 280, L43  
 Coles P., 1993, MNRAS, 262, 1065.  
 Coles P., 1996, Contemp. Phys., 37, 429  
 Coles P., Ellis G.F.R., 1997, Is the Universe Open or Closed? Cambridge University Press, Cambridge  
 Colín P., Carlberg R.G., Couchman H.M.P., 1997, ApJ, 490, 1  
 Connolly A.J., Szalay A.S., Dickinson M., SubbaRao M.U., Brunner R.J., 1997, ApJ, 486, 11  
 Crampton D., Le Fèvre O., Lilly S.J., Hammer F., 1995, ApJ, 455, 96  
 Dekel A., 1986, ComAp, 11, 235  
 Dekel A., Rees M.J., 1987, Nat, 326, 455  
 Efsthathiou G., Frenk C.S., White S.D.M., Davis M., 1988, MNRAS, 235, 715  
 Efsthathiou G., Rees M.J., 1988, MNRAS, 230, 5p  
 Eke V.R., Cole S., Frenk C.S., 1996, MNRAS, 282, 263  
 Ellis R.S., 1997, ARA&A, 35, 389  
 Fry J.N., 1996, ApJ, 461, L65  
 Gheller C., Pantano O., Moscardini L., 1997, MNRAS, in press, astro-ph/9710096  
 Governato F., Baugh C.M., Frenk C.S., Cole S., Lacey C.G., Quinn T., Stadel J., 1997, submitted  
 Hamilton A.J.S., Kumar P., Lu E., Mathews A., 1991, ApJ, 374, L1  
 Hudon J.D., Lilly S.J., 1996, ApJ, 469, 519  
 Jain B., 1997, MNRAS, 287, 687  
 Jain B., Mo H.J., White S.D.M., 1995, MNRAS, 276, L25  
 Jenkins A. et al. 1997, ApJ, submitted, astro-ph/9709010

- Jing Y.P., Suto Y., 1997, preprint, astro-ph/9710090
- Kauffmann G., Nusser A., Steinmetz M., 1997, MNRAS, 286, 795
- La Franca F., Andreani P., Cristiani S., 1997, preprint, astro-ph/9711048
- Le Fèvre O., Hudon D., Lilly S.J., Crampton D., Hammer F., Tresse L., 1996, ApJ, 461, 534
- Lidsey J.E., Coles P., 1992, MNRAS, 258, L57
- Lilje P.B., 1992, ApJ, 386, L33
- Lucchin F., Matarrese S., 1985, Phys. Rev., D32, 1316
- Lucchin F., Matarrese S., Mollerach S., 1992, ApJ, 401, L49
- Matarrese S., Coles P., Lucchin F., Moscardini L., 1997, MNRAS, 286, 115 (Paper I)
- Melott A.L., 1992, ApJ, 393, L45
- Mo H.J., 1997, to appear in Proceedings of Ringberg Workshop on Large-scale Structure, ed. D. Hamilton (Kluwer, Dordrecht), astro-ph/9702218.
- Mo H.J., Fukugita M., 1996, ApJ, 467, L9
- Mo H.J., White S.D.M., 1996, MNRAS, 282, 347
- Mobasher B., Rowan-Robinson M., Georgakakis A., Eaton N., 1996, MNRAS, 282, L7
- Moessner R., Jain B., Villumsen J.V., 1997, MNRAS, in press, astro-ph/9708271
- Munshi D., Chiang L.Y., Coles P., Melott A.L., 1997, MNRAS, in press, astro-ph/9707259
- Munshi D., Padmanabhan T., 1997, MNRAS, 290, 193
- Neuschaefer L.W., Im M., Ratnatunga K.U., Griffiths R.E., Casertano S., 1997, ApJ, 480, 59
- Nusser A., Davis M., 1994, ApJ, 421, L1
- Ogawa T., Roukema B.F., Yamashita K., 1997, ApJ, 484, 53.
- Padmanabhan T., 1996, MNRAS, 278, L29
- Padmanabhan T., Cen R., Ostriker J.P., Summers F.J., 1996, ApJ, 466, 604
- Peacock J.A., 1997a, MNRAS, 284, 885
- Peacock J.A., 1997b, to appear in Proceedings of the KNAW colloquium on The most distant radio galaxies (Reidel), astro-ph/9712068.
- Peacock J.A., Dodds S.J., 1994, MNRAS, 267, 1020
- Peacock J.A., Dodds S.J., 1996, MNRAS, 280, L19 (PD96)
- Peebles P.J.E., 1980, The large-scale structure of the Universe. Princeton University Press, Princeton
- Porciani C., 1997, MNRAS, 290, 639
- Press W.H., Schechter P., 1974, ApJ, 187, 425
- Roche N., Eales S., Hippelein H., 1997, preprint, astro-ph/9711068
- Roukema B.F., Peterson B.A., Quinn P.J., Rocca-Volmerange B., 1997, preprint, astro-ph/9707294
- Sawicki M.J., Lin H., Yee H.K.C., 1997, AJ, 113, 1
- Shepherd C.W., Carlberg R.G., Yee H.K.C., Ellingson E., 1997, ApJ, 479, 82
- Steidel C.C., Giavalisco M., Pettini M., Dickinson M., Adelberger K.L., 1996, ApJ, 462, L17
- Steidel C.C., Adelberger K.L., Dickinson M., Giavalisco M., Pettini M., Kellogg M., 1997, preprint, astro-ph/9708125
- Sugiyama N., 1995, ApJS, 100, 281
- Viana P.T.P., Liddle A.R., 1996, MNRAS, 281, 323
- Villumsen J.V., 1996, MNRAS, 281, 369
- Villumsen J.V., Freudling W., da Costa L.N., 1997, ApJ, 481, 578
- Vittorio N., Matarrese S., Lucchin F., 1988, ApJ, 328, 69
- Wechsler R.H., Gross M.A.K., Primack J.R., Blumenthal G.R., Dekel A., 1997, preprint, astro-ph/9712141
- White M., Viana P.T.P., Liddle A.R., Scott D., 1996, MNRAS, 283, 107
- White S.D.M., 1979, MNRAS, 186, 145
- Williams R.E. et al., 1996, AJ, 112, 1335
- Woods D., Fahlman G.G., 1997, ApJ, 490, 11
- Zel'dovich Ya.B., 1970, A&A, 5, 84